TURUN YLIOPISTON JULKAISUJA
ANNALES UNIVERSITATIS TURKUENSIS

SARJA - SER. D OSA - TOM. 999

MEDICA - ODONTOLOGICA

^{18}F-LABELED PRESYNAPTIC DOPAMINERGIC TRACERS

Synthesis, Radiochemical Analyses, and Preclinical Evaluation of [^{18}F]FDOPA and [^{18}F]CFT

by

Sarita Forsback

TURUN YLIOPISTO
UNIVERSITY OF TURKU
Turku 2012

From

Turku PET Centre and Department of Clinical Physiology and Nuclear Medicine**,** University of Turku**,** Turku, Finland

Supervised by

Professor Olof Solin, PhD
Turku PET Centre
University of Turku
Turku, Finland

Docent Merja Haaparanta-Solin, PhD
Turku PET Centre
University of Turku
Turku, Finland

Reviewed by

Dr. Eeva-Liisa Kämäräinen, PhD
Department of Clinical Physiology and Nuclear Medicine
Helsinki University Central Hospital
Helsinki, Finland

Dr. Jacek Koziorowski, PhD
Department of Clinical Physiology 54P1
Herlev University Hospital
Herlev, Denmark

Dissertation opponent

Professor Jörg Steinbach, PhD
Helmholtz-Zentrum Dresden-Rossendorf
Institute of Radiopharmacy
Dresden, Germany

ISBN 978-951-29-4844-4 (PRINT)
ISBN 978-951-29-4845-1 (PDF)
ISSN 0355-9483
Painosalama Oy – Turku, Finland 2012

To my family

Cover illustration: [^{18}F]CFT PET/CT image of a healthy rat. Clearly localized accumulation of ^{18}F-activity is seen in striatum of brain (colour scale; red high uptake, blue low uptake). Anatomical delineation is provided by the overlaid CT image (grayscale).

ABSTRACT

Sarita Forsback

^{18}F-LABELED PRESYNAPTIC DOPAMINERGIC TRACERS
Synthesis, Radiochemical Analyses, and Preclinical Evaluation of [^{18}F]FDOPA and [^{18}F]CFT

Turku PET Centre and Department of Clinical Physiology and Nuclear Medicine, University of Turku, Turku, Finland

Annales Universitatis Turkuensis
Painosalama Oy, Turku, Finland 2012

Dysfunction of the dopaminergic system in brain is involved in several pathological conditions such as Parkinson's disease and depression. 2β-Carbomethoxy-3β-(4-[^{18}F] fluorophenyl)tropane ([^{18}F]CFT) and 6-[^{18}F]fluoro-L-dopa ([^{18}F]FDOPA) are tracers for imaging the dopaminergic function with positron emission tomography (PET). Peripheral uptake of [^{18}F]FDOPA is also used in the localization and diagnosis of neuroendocrine tumors.

[^{18}F]FDOPA and [^{18}F]CFT can be synthesized by electrophilic fluorodestannylation. However, the specific radioactivity (SA) in the electrophilic fluorination is low with traditional synthetic methods. In this study, [^{18}F]FDOPA and [^{18}F]CFT were synthesized using post-target-produced [^{18}F]F_2 as an electrophilic fluorination agent. With this method, tracers are produced with sufficient SA for neuroreceptor studies. Specific aims in this study were to replace Freon-11 in the production of [^{18}F]FDOPA due to the ozone depleting properties of this solvent, to determine pharmacological specificity and selectivity of [^{18}F]CFT with respect to monoamine transporters, and to compare the ability of these tracers to reflect the degree of nigral neuronal loss in rats in which the dopaminergic system in the brain had been unilaterally destroyed by 6-OHDA.

Post-target-produced [^{18}F]F_2 was successfully used in the production of [^{18}F]FDOPA and [^{18}F]CFT. The SA achieved was substantially higher than in previous synthetic methods. Deuterated compounds, CD_2Cl_2, $CDCl_3$ and C_3D_6O, were found to be suitable solvents for replacing Freon-11. Both [^{18}F]FDOPA and [^{18}F]CFT demonstrated nigrostriatal dopaminergic hypofunction and correlated with the number of nigral dopaminergic neurons in the 6-OHDA lesioned rat. However, the dopamine transporter (DAT) tracer [^{18}F]CFT was more sensitive than the dopamine synthesis tracer [^{18}F]FDOPA in detecting these defects because of the higher non-specific uptake of [^{18}F]FDOPA. [^{18}F]CFT can also be used for imaging the norepinephrine transporter (NET) because of the specific uptake into the locus coeruleus. The observation that [^{18}F]CFT exhibits specific uptake in the pancreas warrants further studies in humans with respect to potential utility in pancreatic imaging.

Key words: electrophilic fluorodestannylation, post-target-produced [^{18}F]F_2 dopaminergic system, [^{18}F]FDOPA, [^{18}F]CFT, DAT, NET, positron emission tomography.

TIIVISTELMÄ

Sarita Forsback

^{18}F-LEIMATUT PRESYNAPTISTA DOPAMINERGISTÄ JÄRJESTELMÄÄ KUVANTAVAT MERKKIAINEET
[^{18}F]FDOPA:n ja [^{18}F]CFT:n valmistus, radioanalyyttiset määritykset ja arviointi koe-eläimessä.

Valtakunnallinen PET-keskus ja Kliininen fysiologia ja isotooppilääketiede, Turun yliopisto, Turku

Annales Universitatis Turkuensis
Painosalama OY, Turku, Finland 2012

Useissa tautitiloissa, kuten esimerkiksi Parkinsonin taudissa ja masennuksessa, voidaan havaita aivojen dopaminergisen järjestelmän muutoksia. 2β-karbometoksi-3β-(4-[^{18}F]fluorifenyyli)tropaani ([^{18}F]CFT) ja 6-[^{18}F]fluori-L-dopa ([^{18}F]FDOPA) ovat radioaktiivisia merkkiaineita, joiden avulla dopaminergistä järjestelmää voidaan kuvantaa positroniemissiotomografialla (PET).

[^{18}F]FDOPA ja [^{18}F]CFT voidaan syntetisoida käyttämällä elektrofiilistä fluoridestannylaatiota. Menetelmän haittapuolena on kuitenkin lopputuotteen matala ominaisradioaktiivisuus (OR). Tämän työn tavoitteena oli valmistaa [^{18}F]FDOPA:a ja [^{18}F]CFT:tä käyttäen elektrofiilisena leimausaineena sähköpurkauksen avulla tuotettua [^{18}F]F_2-kaasua. Näin valmistettujen merkkiaineiden OR on riittävän korkea neuroreseptoritutkimuksiin. Lisäksi tavoitteina oli korvata fluorausreaktiossa yleisesti käytetty ilmakehää tuhoava freon-11 vähemmän haitallisella liuottimella, tutkia [^{18}F]CFT:n sitoutumista monoamiini-välittäjäaineisiin ja verrata [^{18}F]FDOPA:n ja [^{18}F]CFT:n kykyä kuvantaa rotan aivojen mustatumakkeen hermosolujen vähenemistä dopaminergisen järjestelmän vaurion jälkeen.

Sähköpurkauksen avulla tuotettu [^{18}F]F_2 soveltui hyvin [^{18}F]FDOPA:n ja [^{18}F]CFT:n valmistukseen. Haitallinen Freon-11 voitiin korvata deuteroiduilla dikloorimetaanilla, kloroformilla tai asetonilla. Rotan aivoissa sekä [^{18}F]FDOPA- että [^{18}F]CFT-injektioiden jälkeen mitattu radioaktiivisuuskertymä oli verrannollinen dopaminergisen järjestelmän vaurion jälkeen jäljelle jääneiden mustatumakkeen hermosolujen määrään. [^{18}F]CFT, joka kuvantaa dopamiinin kuljetusproteiinien toimintaa solussa, oli herkempi havaitsemaan tätä hermosolujen määrän vähenemistä kuin dopamiinin synteesiä kuvantava [^{18}F]FDOPA, koska [^{18}F]CFT:n epäspesifinen radio-aktiivisuuskertymä on aivoissa alhaisempi kuin [^{18}F]FDOPA:n. Spesifistä radio-aktiivista kertymää löydettiin [^{18}F]CFT-injektion jälkeen myös rotan aivojen locus coeruleus-tumakkeesta, joka on noradrenergisen hermojärjestelmän päätumake aivorungossa, ja haimasta. Näin ollen [^{18}F]CFT saattaisi soveltua myös noradrenaliinin kuljetuksen ja haiman toiminnan kuvantamiseen.

Avainsanat: elektrofiilinen fluoridestannylaatio, sähköpurkauksen avulla tuotettu [^{18}F]F_2, dopaminerginen järjestelmä, [^{18}F]FDOPA, [^{18}F]CFT, positroniemissiotomagrafia.

CONTENTS

ABBREVIATIONS

AADC	aromatic L-amino acid decarboxylase
AD	aldehyde dehydrogenase
ANOVA	repeated-measurement analysis of variance
(S)-Boc-BMI	(S)-(-)-1-Boc-2-t-butyl-3-methyl-4-imidazolidinone
[^{76}Br]CBT	2β-carbomethoxy-3-β-(4-[^{76}Br]bromophenyl)tropane
$CDCl_3$	deuterated chloroform
CD_2Cl_2	deuterated dichloromethane
C_3D_6O	deuterated acetone
[^{18}F]CFT	2β-carbomethoxy-3-β-(4-[^{18}F]fluorophenyl)tropane
[^{18}F]CH_3COOF	acetyl [^{18}F]hypofluorite
[^{123}I]CIT	2β-carbomethoxy-3-β-(4-[^{123}I]iodophenyl)tropane
$CHCl_3$	chloroform
CH_2Cl_2	dichloromethane
C_3H_6O	acetone
COMT	cathecol-*O*-methyl transferase
DABCO	1,4-diazabicyclo[2,2,2]octane
DAT	dopamine transporter
DOPA	3,4-dihydroxyphenylalanine
[^{11}C]DTBZ	[^{11}C]dihydroxytetrabenazine
ED	effective dose
EOB	end of bombardment
EOS	end of synthesis
[^{18}F]FDG	2-deoxy-2-[^{18}F]fluoro-D-glucose
[^{18}F]FDOPA	6-[^{18}F]fluoro-L-dopa
[^{18}F]FDOPAC	3,4dihydroxy-6-[^{18}F]fluorophenylacetic acid
[^{18}F]FE-PE2I	[^{18}F](E)-N-(3-iodoprop-2-enyl)-2β-carbofluoro-ethoxy-3β-(4'-methyl-phenyl) nortropane
[^{18}F]FHVA	6-[^{18}F]fluorohomovanillic acid
[^{18}F]FMT	6-[^{18}F]fluoro-L-*m*-tyrosine
Freon-11	CCl_3F, trichlorofluoromethane
HPLC	high performance liquid chromatography
LC	locus coeruleus

LC/MS	liquid chromatography mass spectrometry
MAO	monoamine oxidase
3-[^{18}F]MFT	3-*O*-methoxy-6-[^{18}F]fluorotyramine
MPTP	1-methyl-4-phenyl-1,2,3,6-tetrahydropyridine
NCA	no-carrier-added
NET	norepinephrine transporter
(S)-NOBIN	2-amino-2'-hydroxy-1,1'-binaphtyl
NiPBPGly	Ni(II) complex of a Schiff base of (*S*)-*O*-[(*N*-benzylpropyl)amino]benzophenone and glycine
[^{18}F]OF_2	oxygen [^{18}F]difluoride
6-OHDA	6-hydroxy dopamine
OLINDA	organ level internal dose assessment code
3-[^{18}F]OMFD	3-*O*-methyl-6-[^{18}F]fluoro-L-dopa
[^{11}C]PE2I	[^{11}C]N-(3-iodoprop-2-enyl)-2beta-carbomethoxy-3beta-(4-methylphenyl)nortropane
PET	positron emission tomography
PD	Parkinson's disease
PSL	photostimulated luminescence
PST	phenolsulfotransferase
PTC	phase-transfer catalyst
QC	quality control
RCP	radiochemical purity
RCY	radiochemical yield
[^{11}C]RTI-31	[*N*-^{11}C]2β-carbomethoxy-3-β-(4-chlorophenyl)tropane
SA	specific radioactivity
SD	standard deviation
SERT	serotonine transporter
SN	substantia nigra
SPECT	single-photon emission computerized tomography
TH	tyrosine hydroxylase
TLC	thin layer chromatography
UV	ultraviolet
VMAT	vesiclar monoamine transporter

LIST OF ORIGINAL PUBLICATIONS

This thesis is based on the following original publications, which are referred to in the text by their Roman numerals.

I Forsback S, Eskola O, Haaparanta M, Bergmann J and Solin O. Electrophilic synthesis of 6-[^{18}F]fluoro-L-DOPA using post-target produced [^{18}F]F2. Radiochim Acta 2008; 96:845-848.

II Forsback S, Eskola O, Bergman J, Haaparanta M, Solin O. Alternative solvents for electrophilic synthesis of 6-[^{18}F]fluoro-L-DOPA. J Label Compd Radiopharm 2009; 52:286-288.

III Forsback S, Marjamäki P, Eskola O, Bergman J, Rokka J, Haaparanta M, Solin O. [^{18}F]CFT, synthesis and binding to monoamine transporters in rat. In press, EJNMMI Research.

IV Forsback S, Niemi R, Marjamaki P, Eskola O, Bergman J, Gronroos T, Haaparanta M, Haapalinna A, Rinne J, Solin O. Uptake of 6-[^{18}F]fluoro-L-dopa and [^{18}F]CFT reflect nigral neuronal loss in a rat model of Parkinson's disease. Synapse 2004; 51:119-27.

 In addition, unpublished data are presented in this thesis.

1. INTRODUCTION

Positron emission tomography (PET) with specific radiopharmaceuticals is a unique molecular imaging modality for quantitative study of functional processes and biochemical parameters such as the dopaminergic system in living subjects. The required radiopharmaceuticals are labeled with a positron emitter, most often with carbon-11 (^{11}C) or fluorine-18 (^{18}F). An ideal radiopharmaceutical has high affinity and selectivity for the target, low non-specific binding, and suitable pharmacokinetics in relation to the half-life of the radionuclide. Additionally, the metabolism of the radiopharmaceutical must be insignificant or well characterized, because the PET method does not identify the chemical source of the radioactivity. The specific radioactivity (SA) must be high enough to avoid pharmacological effects in the study subjects.

^{18}F (half-life 109.8 min) is one of the most common positron emitters used in PET radiochemistry. Fluorine is the most electronegative element and is increasingly used in drugs (Park and Kitteringham 1994, Strunecká et al. 2004), although it is uncommon in organic compounds in nature. Fluorine can be used to substitute a hydrogen atom or a hydroxyl group in a drug molecule, but the substitution will affect the physical, chemical, and biological properties of the molecule. Fluorine substitution can improve the selectivity and the efficacy of a drug, or the substitution can ease drug administration (Park and Kitteringham 1994). Carbon is an organic element, and ^{11}C is widely used in PET radiopharmaceuticals by substituting for inactive carbon; however, the short half-life (20.4 min) of ^{11}C may limit its use in PET. On the other hand, this short half-life offers the possibility of studying one subject with several ^{11}C tracer injections in a single day. Despite the high theoretical SA, the SA of ^{11}C-labeled radiopharmaceuticals suffers from the wide natural abundance of carbon and from the decline of the SA with the half-life. The evaluation of the uptake and distribution of a radiopharmaceutical in healthy experimental animals or in animal disease models provides important information prior to the inception of human studies, for example regarding the pharmacokinetics of the radiopharmaceutical and the stability of the label.

Dopamine is the predominant catecholamine neurotransmitter in the brain. It is mainly enriched in the striatum and substantia nigra (SN), but also occurs in the peripheral nerves to some extent (Bell 1989). Several pathological conditions such as Parkinson's disease (PD), depression, and schizophrenia are known to be related to dysfunction of the dopaminergic system, which also participates in addiction development and is thought to regulate insulin secretion (Ichise and Harris 2010).

This study focused on two radiopharmaceuticals, 2β-carbomethoxy-3β-(4-[^{18}F]fluorophenyl)tropane ([^{18}F]CFT) and 6-[^{18}F]fluoro-L-dopa ([^{18}F]FDOPA), which are used to image different aspects of the dopaminergic system. The purpose of the current investigation was to improve the electrophilic labeling chemistry of the

radiopharmaceuticals and to compare their brain uptake in healthy rats and in an animal model of PD. The biodistribution of [^{18}F]CFT and its affinity to monoamine transporters were also studied.

2. REVIEW OF THE LITERATURE

2.1. Production of ^{18}F-labeled radiopharmaceuticals

2.1.1. Production of $[^{18}F]F^-$ and $[^{18}F]F_2$

Cyclotron acceleration of charged particles with subsequent nuclear reactions is the preferred method to produce short-lived positron-emitting radionuclides (Mason and Mathis 2003). The most common method to produce nucleophilic fluoride, $[^{18}F]F^-$, is the $^{18}O(p,n)^{18}F$ nuclear reaction using highly enriched $[^{18}O]H_2O$ as target material (Table 2.1., Ruth and Wolf 1979, Solin et al. 1988). This high-yield reaction generates close to terabequerel amounts at the low proton energies (<16 Mev) achieved by the most commonly used cyclotrons (Guillaume et al. 1991). ^{18}F is obtained as an aqueous solution, no-carrier-added (NCA), and with a high SA up to 5,000 GBq/μmol (Solin et al. 1988), but the solvated $[^{18}F]F^-$ is quite unreactive. Ion reactivity is enhanced by addition of a cationic counterion such as potassium carbonate Kryptofix222 complex prior to the azeotropic evaporation of the water with acetonitrile (Schirrmacher et al. 2010).

Two nuclear reactions, $^{20}Ne(d,\alpha)^{18}F$ (Lambrecht et al. 1978) and $^{18}O(p,n)^{18}F$ (Ruth and Wolf 1979), are currently used to produce electrophilic fluorine $[^{18}F]F_2$ (Table 2.1.). The $^{20}Ne(d,\alpha)^{18}F$ nuclear reaction employs neon gas as a target with added F_2 to maintain the fluorine as molecular fluorine (Casella et al. 1980). $[^{18}F]F_2$ is removed from the target in neon together with radioactive impurities such as $[^{18}F]NF_3$ and $[^{18}F]CF_4$ and can be directly used for synthesis. The $^{18}O(p,n)^{18}F$ nuclear reaction utilizes $^{18}O_2$ gas as a target material (Nickles et al. 1983, 1984, Chirakal et al. 1995). $^{18}O_2$ is removed after irradiation and to recover ^{18}F as $[^{18}F]F_2$ the target is filled with F_2 gas mixed in a noble gas. The target is irradiated briefly and the gas mixture, including the $[^{18}F]F_2$ formed in an exchange reaction with ^{18}F attached to the target chamber walls, is removed and used in synthesis directly (Nickles et al. 1984). The oxygen reaction is three to five times more efficient than the neon reaction due to the nuclear reaction cross sections for the particular production methods (Ruth and Wolf 1979). This holds for the particle energy ranges for commonly used cyclotrons in PET radionuclide production. The SA of $[^{18}F]F_2$ achieved by gaseous $^{18}O(p,n)^{18}F$ is higher (1.3 GBq/μmol, Chirakal et al. 1995) than the SA of the $[^{18}F]F_2$ produced by the $^{20}Ne(d,\alpha)^{18}F$ reaction (0.05-0.1 GBq/μmol, Blessing et al. 1986). Moreover, modern low-energy (10-18 MeV) PET cyclotrons are mostly operated with proton beams, with some inconvenience in switching to deuteron beams. The use of the $^{18}O(p,n)^{18}F$ nuclear reaction is preferred over the $^{20}Ne(d,\alpha)^{18}F$ nuclear reaction even though the neon reaction is still more commonly used. Both methods produce low yields of $[^{18}F]F_2$ (<37GBq) and they suffer from low SA due to the high amount (40-60 μmol) of carrier F_2. $[^{18}F]F_2$ produced by these nuclear reactions is not appropriate for labeling the radiotracers that easily saturate receptor sites or that are toxic.

Table 2.1. Selected nuclear reactions for the production of ^{18}F-labeled precursors.

Nuclear reaction	Target material	^{18}F-labeled precursor	SA [GBq/μmol]
^{18}O(p,n)^{18}F	$H_2{}^{18}O$	$[^{18}F]F^-$	5000
^{20}Ne(d,α)^{18}F	Ne + F_2	$[^{18}F]F_2$	0.05-0.1
^{18}O(p,n)^{18}F	$^{18}O_2$ + F_2	$[^{18}F]F_2$	1.3
^{18}O(p,n)^{18}F	$H_2{}^{18}O$	Post-target produced $[^{18}F]F_2$	55

$[^{18}F]F^-$; nucleophilic fluorinating reagent
$[^{18}F]F_2$; electrophilic fluorinating reagent

In order to improve the SA of the electrophilic ^{18}F-labeled precursor, post-target production of $[^{18}F]F_2$ was developed (Bergman and Solin 1997), which utilizes the aqueous $^{18}O(p,n)^{18}F$ nuclear reaction. Azeotropically dried $[^{18}F]F^-$ is reacted with methyl iodide (CH_3I) in dry acetonitrile to generate methyl $[^{18}F]$fluoride ($[^{18}F]CH_3F$), which is purified by gas chromatography. Purified $[^{18}F]CH_3F$ is then transferred to a discharge chamber with a small, controllable amount (0.15-1 μmol) of carrier F_2 in neon. The mixture is atomized by an electrical discharge (35 kV, 400 μA, 10 s) after which a rearrangement and $^{18}F/^{19}F$ exchange produce $[^{18}F]F_2$. The SA and the yield of $[^{18}F]F_2$ correlate with the amounts of $[^{18}F]CH_3F$ and carrier F_2 used, as well as with the efficiency of the $^{18}F/^{19}F$ exchange. An SA of 55 GBq/μmol was achieved with 0.15 μmol of carrier F_2 and 7.5 GBq of $[^{18}F]F_2$ (Bergman and Solin 1997).

^{18}F can be incorporated into a molecule by nucleophilic or electrophilic methods (reviewed by Lasne et al. 2002, Schlyer 2004, Schirrmacher et al. 2007). The short half-life and the high level of radioactivity of the starting material distinguish the labeling chemistry from traditional organic chemistry. Due to the high radioactivity of the labeling procedure, the purification and the formulation of the radiopharmaceutical must be rapid and automated, or at least remote-controlled. It is preferable that the radionuclide is introduced into the molecule during the last step of radiotracer preparation in order to achieve the highest possible radiochemical yield (RCY, Coenen 2007). The stoichiometry of the radiolabeling reaction also differs from traditional organic chemistry, as the amount of cyclotron-produced radionuclide is in the low nanomolar range, while all other reactants are used in large excess and even small impurities may disturb the reaction. Radiotracers that easily saturate the receptor or target sites or that are toxic limit the labeling chemistry; the radiotracers must be obtained with high SA in order to minimize the injected amount per study subject.

2.1.2. Nucleophilic fluorination

The majority of ^{18}F-labeled radiotracers are produced by nucleophilic fluorination, at least in part due to the easier availability of $[^{18}F]F^-$ compared to $[^{18}F]F_2$. Nucleophilic fluorination is divided into two principal categories. In the first category, aliphatic

precursors containing leaving groups such as halides or alkyl sulfonate esters are labeled using aliphatic nucleophilic displacement. The second category, aromatic nucleophilic substitution, utilizes activated aromatic systems with leaving groups such as nitro or trimethylammonium (Lasne et al. 2002, Mason and Mathis 2003, Schlyer 2004, Coenen 2007, Cai et al. 2008). Incorporation of the label directly into the aromatic ring generally offers good metabolic stability of ^{18}F-labeled compounds, a major advantage in PET imaging. Both aliphatic nucleophilic displacement and aromatic nucleophilic substitution are usually carried out in polar aprotic solvents, most commonly in acetonitrile, and can be performed either directly on a suitable precursor or indirectly via a labeled prosthetic group such as [^{18}F]-fluorinated alkyl or benzyl halides. Direct labeling with [^{18}F]F$^-$ often leads to poor RCY and the use of labeled prosthetic groups can be complicated and time-consuming, requiring multistep synthesis (Lasne et al. 2002). New methods such as enzymatic fluorination and click chemistry have been developed and used to achieve more complex radiofluorinated compounds (Schirrmacher 2007, Cai et al. 2008).

2.1.3. Electrophilic fluorination

Electrophilic fluorination was successfully carried out in the early years of PET radiochemistry, but its use is limited due to the low SA of the electrophilic labeling agents. Half of the radioactivity is lost during the production of monofluorinated products. In addition, [^{18}F]F_2 is very reactive, leading to low selectivity and often to undesired side reactions (sensitive functional groups of a precursor must be protected). Thus, the development of high-yield [^{18}F]F$^-$ production methods and stereospecific nucleophilic radiofluorination have decreased the use of electrophilic labeling. However, electrophilic labeling offers a method for the [^{18}F]-fluorination of electron-rich compounds, which are unavailable through nucleophilic labeling. Electrophilic labeling is also faster and more easily automated than nucleophilic labeling; product is achieved by bubbling [^{18}F]F_2 with a noble gas through a reaction vessel containing an appropriate precursor dissolved in a suitable solvent. Aromatic electrophilic substitution is the most-used electrophilic reaction. Aliphatic electrophilic addition to a double bond is also useful, but seldom implemented (Dolbier Jr. et al. 2001, Eskola et al. 2011).

The selectivity of electrophilic labeling has been improved via demetallation reactions of organometallic precursors; suitable precursors include aryltrimethyltin, aryltrimethylgermanium and arylmethylsilicon compounds. The highest regiospecific fluorination yields were obtained using organotin moieties (Coenen and Moerlein 1987). Mercurated precursors have also been used in demetallation reactions (Adam and Jivan 1988, Luxen et al. 1990).

To decrease the reactivity of [^{18}F]F_2, various fluorinating agents have been synthesized. Acetyl [^{18}F]hypofluorite ([^{18}F]CH_3COOF, Fowler et al. 1982) is the most common agent, and other compounds such as xenon[^{18}F]difluoride ([^{18}F]XeF_2, Chirakal et al.

1984a), [^{18}F]fluoro-2-pyridone (Oberdorfer et al. 1988), and *N*-[^{18}F]fluoro-*N*-alkylsulfonamides (Satyamurthy et al. 1990) have been tested but are not widely used. Low yield and poor reproducibility have prevented the use of NCA [^{18}F]perchloryl fluoride (Hiller et al. 2008). A novel [^{18}F]NF reagent, [^{18}F]-*N*-fluorobenzenesulfonimide, has also been prepared and used for the synthesis of ^{18}F-labeled compounds (Teare et al. 2007). More recently, the preparation of [^{18}F]selectfluor *bis*(triflate) and its usefulness in the preparation of clinically used radiotracers has been presented (Teare et al. 2010). The development of stable, reactive, and selective electrophilic ^{18}F-fluorination agents will most like advance electrophilic ^{18}F-labeling technology in the future.

2.1.4. Quality of radiopharmaceuticals

Radiopharmaceuticals are considered to be a special group of drugs. Most radiopharmaceuticals are administered intravenously, and their manufacturing and use are regulated by even stricter regulations than traditional drugs (Elsinga et al. 2010). In addition, the short half-lives and low masses of radiopharmaceuticals mandate special requirements for quality control (QC, Vallabhajosula 2009). The European Association of Nuclear Medicine has published practice-oriented guidelines for good radiopharmacy practice for small-scale non-commercial preparation of radiopharmaceuticals (Elsinga et al. 2010). General recommendations for the preparation of radiopharmaceuticals in Europe are presented in the European Pharmacopoeia (7th Edition), which includes specific monographs for common radiopharmaceuticals such as [^{18}F]FDOPA. These monographs provide detailed instructions regarding the quality control of a given radiopharmaceutical.

The manufacturing process, including preparation and QC, must be validated before routine production to guarantee the robustness and reliability of the process. QC tests include visual examination of the appearance of the final product (color, clearness), measurement of the pH, analyses of identity, radionuclidic purity, chemical purity (including stereomeric and enantiomeric purity), radiochemical purity (RCP), sterility, endotoxins, stability, residual solvents, and other possibly toxic chemicals used during synthesis. Combinations of the QC tests are performed from every production run before the tracer is released for human use. High performance liquid chromatography combined to radioactivity detector (radioHPLC) and thin layer chromatography (TLC) analyzed for radioactivity by digital autoradiography are the most common routine QC methods for testing identity, RCP, and chemical purity. Some QC tests such as the analyses of stability, sterility, endotoxins, residual solvents, and other toxic chemicals can be performed only during validation or from selected production runs on a regular basis.

2.1.5. Specific radioactivity (SA)

A PET radioligand suitable for *in vivo* neuroreceptor studies must have moderate to high SA to avoid saturation of receptor sites and to avoid pharmacological effects in study subjects. For [^{18}F]FDOPA which is a fluorinated analogue of endogenous DOPA, high SA is not as important. The SA is usually presented as the amount of radioactivity per molar mass (GBq/μmol). It is important to specify the time point at which the SA is defined, since the SA is reduced in relation to the physical decay of the radionuclide. Maximum SA is not achievable for the most common PET radionuclides such as ^{11}C and ^{18}F, given the wide abundance of their stable isotopes and subsequent contamination with stable material. ^{19}F contamination mainly originates from the target and target chamber material (Solin et al. 1988) and from the material of the transportation lines (Füchtner et al. 2008, Berridge at al. 2009). The use of inactive carrier in the production of a radionuclide or in the synthesis of a radioligand also decreases the SA drastically. The SA is commonly determined using radioHPLC combined with ultraviolet (UV) absorption detection by comparing the peak intensities of the final product and the peak intensities of the reference compound of known concentration and radioactivity concentration. For radioligands with very high SA, limitation of the sensitivity of UV detection requires the use of other methods such as liquid chromatograpy mass spectrometry (LC/MS, Solin et al 2004) or HPLC with fluorescence detection (Nakao et al. 2008).

2.2. Measurement of radioactivity

Radioactive decay is the process by which an atomic nucleus of an unstable atom loses energy by emitting ionizing particles (ionizing radiation). This decay is a random process that releases energy and matter from the nucleus. Detection of radioactivity is based on the interaction of the released energy with a detector; the energy of radiation can be converted to electric current by ionization of gas molecules or by excitation and ionization of solid or liquid scintillator material. Dose calibrators, pocket dosimeters, and Geiger-Müller counters are typical gas-filled detectors. Sodium iodide crystal with a small amount of thallium (NaI(Tl)) is widely used scintillator that is utilized in well counters or in combination with HPLC.

2.2.1. Positron emission tomography (PET)

Positron-emitting radionuclides decay by emitting the antiparticles of electrons, positrons (β^+), which annihilate electrons after traversing a certain range depending on media density, resulting in two 511-keV gamma signals having a relative angle of 180° (Paans et al. 2002). These simultaneous signals are registered by a ring of scintillation detectors around a subject inside a PET scanner. The range of the positron depends on its energy and affects image resolution. The positron energy of ^{18}F is low, offering better resolution than other widely used PET radionuclides (Table 2.2).

Table 2.2. Physical properties of positron emitters.

Nuclide	Half-life	Type of decay	Maximum endpoint β-energy [keV]	Maximum range in H_2O [mm]	Max. SA [TBq/μmol]
^{15}**O**	2.03 min	β^+ (99.9%)	1732	8.0	3390
^{13}**N**	9.97 min	β^+ (99.9%)	1198	5.1	699
^{11}**C**	20.4 min	β^+ (99.8%)	960	3.9	341
^{68}**Ga**	67.7 min	β^+ (87.9%)	1899	8.9	103
^{18}**F**	109.8 min	β^+ (96.7%)	634	2.3	63
^{64}**Cu**	12.1 h	β^+ (17.4%)	653	2.4	9.1
^{124}**I**	4.18 d	β^+ (22.8%)	2138	10.2	1.2

National Nuclear Data Center, Brookhaven National Laboratory, Upton, NY 11973-5000

PET provides quantitative measures of biochemical parameters such as the concentration and function of transporters and enzymes in living subjects. One advantage of PET is the capability of performing kinetic analysis of radioactivity accumulation in a single experimental subject over time. Preclinical PET studies with radiotracers that are already in clinical use can lead to further understanding of the molecular pathology of animal models of human diseases (Jacobs et al. 2003). PET is increasingly implemented in drug discovery, for example to confirm mechanism of action, to guide the selection of clinical dose, and to monitor the response to drug treatment (Lee and Farde 2006).

2.2.2. Digital autoradiography

Despite progress in the development of dedicated small animal PET scanners (Hume and Myers 2002, Schnöckel et al. 2010), preclinical studies still suffer from the low spatial resolution of PET. The resolution of commonly used animal PET scanners is 1-2 mm. Autoradiography using storage phosphor technology (Johnston et al. 1990) is the method of choice for supporting *in vivo* preclinical studies. This type of digital autoradiography offers excellent linearity, sensitivity, and resolution up to 25 μm, and thus it can be used to analyze the radioactivity distribution even in small structures with low radioactivity in an experimental animal. In digital autoradiography, thin slices from a target organ are exposed to a storage phosphor plate, the radioactive decay in the cryosections excites the phosphor crystals on the plate, and the excited plate is stimulated with a laser to release the stored energy as photostimulated luminescence (PSL). The PSL values of rat brain sections have an excellent linear relationship with the radioactivity over a wide range under constant slide thickness (Ishiwata et al. 1999). Digital autoradiography combined with thin layer chromatography is a very sensitive method for investigating the metabolism of radiopharmaceuticals (Haaparanta et al. 2004).

2.2.3. Dosimetry

Radiation dosimetry is the calculation of the absorbed dose in matter and tissue resulting from the exposure to indirectly and directly ionizing radiation. The dose is presented as an effective dose (ED). The ED is the tissue-weighted sum of the equivalent doses in tissues and organs of the body, accounting for the type of radiation. The ED is calculated using programs such as OLINDA (Organ Level Internal Dose Assessment Code, Vanderbilt University, Nashville, TN, USA, Stabin et al. 2005) and the SI unit of both measures is the sievert (Sv, J/kg). Radiation doses are usually expressed as Sv/MBq; the ED from one 2-deoxy-2-[^{18}F]fluoro-D-glucose ([^{18}F]FDG) injection is approximately 20 μSv/MBq (Johansson et al. 1992). ED also depends on the half-life of the radiation source, and thus the doses of ^{11}C-labeled radiopharmaceuticals tend to be lower than the doses of ^{18}F-labeled radiopharmaceuticals. An ED up to 10 mSv per study is acceptable for healthy volunteers if the study has substantial benefit to society (The 2007 Recommendations of the International Commission on Radiological Protection, ICRP).

2.3. Presynaptic dopaminergic system

Neurotransmitters such as dopamine are chemicals that transmit signals from one nerve cell to another; they are produced in and localized to presynaptic terminals, then stored in synaptic vesicles by vesicular transport (Fig. 2.1.). Neurotransmitters are released following an adequate electrical signal, inducing postsynaptic effects in target cells. Neurotransmitters are rapidly inactivated after release by specific enzymes or by re-uptake to prevent further excitatory or inhibitory signal transduction (von Bohlen und Halbach and Dermietzel 2006).

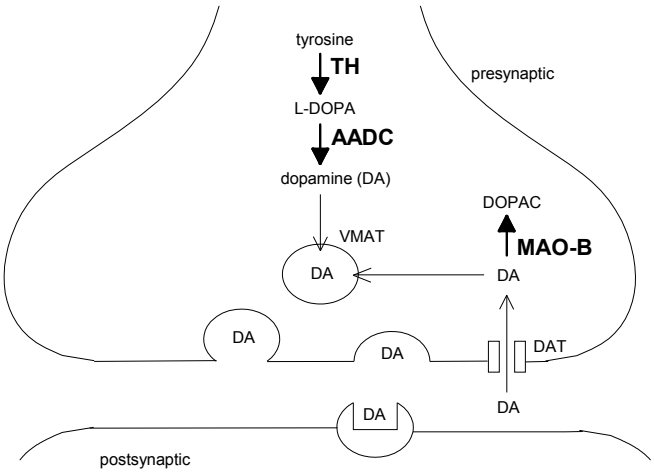

Figure 2.1. Schematic representation of a dopaminergic presynaptic terminal.. Figure is modified from Cooper et al. 1996. (DOPAC = 3,4-Dihydroxyphenylacetic acid)

2.3.1. Dopamine

The function of dopamine as a neurotransmitter was reported in 1958 (Carlsson et al 1958). Prior to that investigation, dopamine was thought to be only an intermediate product in norepinephrine synthesis. Dopamine is synthesized from the amino acid precursor tyrosine to 3,4-dihydroxyphenylalanine (DOPA) by tyrosine hydroxylase (TH) and then by aromatic L-amino acid decarboxylase (AADC) to dopamine (Fig. 2.2). Dopamine is a necessary precursor of norepinephrine, and in noradrenergic neurons, dopamine is further synthesized to norepinephrine.

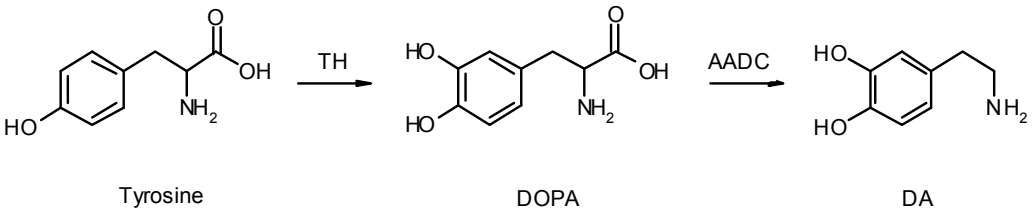

Figure 2.2. Dopamine (DA) synthesis.

The main dopaminergic pathways in the brain are presented in Fig. 2.3.. The mesocortical and mesolimbic pathways originate from the ventral tegmental area and are projected to several cortical areas, the septum, and the olfactory bulb or to the nucleus accumbens via the amygdala and the hippocampus, respectively. The nigrostriatal pathway runs from the SN to the striatum. The tuberoinfundibular pathway connects the hypothalamus to the pituitary gland. In addition, there are small projections to the locus coeruleus (LC) and to the spinal cord. LC is situated in the brain stem (not shown in the Fig. 2.3.) Abnormal activity of the mesocortical and the mesolimbic pathways is known to affect psychiatric symptoms such as schizophrenia, and the loss of dopaminergic neurons in the nigrostriatal pathway is the main cause of the development of PD (von Bohlen und Halbach and Dermietzel 2006).

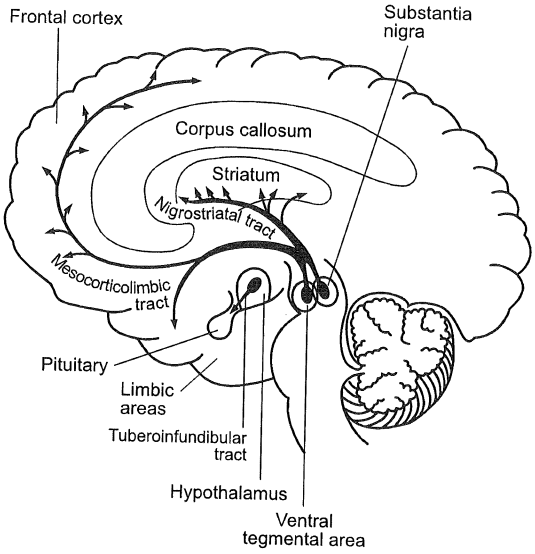

Figure 2.3. The main dopaminergic pathways in the brain. Figure is modified from Andreasen 1988.

2.3.2. Dopamine storage and re-uptake

After synthesis, dopamine is taken up from the cytoplasm by vesicular monoamine transporters (VMATs) and stored in synaptic vesicles (Fig. 2.1). VMATs are divided into two subgroups: VMAT1 is predominantly found in endocrine and paracrine cells in the peripheral organs, and VMAT2 is expressed mainly in neurons and in some endocrine populations such as the pancreas (Iversen 2000, Zheng et al. 2006, Wimalasena 2011).

The dopamine transporter (DAT, Fig. 2.1.), a presynaptically located protein, plays an important role in the inactivation of the dopaminergic signal in the synaptic cleft, and it is the major target of psychostimulant drugs (Eisenhofer 2001, Piccini 2003, Torres et al. 2003). Released dopamine can also be taken up again by the norepinephrine transporter (NET, Morón et al. 2002), but DAT exclusively occurs in dopamine neurons and seems to be a defining characteristic of dopamine neurons (Piccini 2003). DAT is principally expressed in the SN, striatum, and ventral tegmental area (Torres et al. 2003), and is also found peripherally in the stomach, pancreas, and kidney (Eisenhofer 2001).

2.3.3. PET radiotracers for the presynaptic dopaminergic system

PET-based investigations of the presynaptic dopaminergic function have focused on dopamine synthesis, transport inside the cell in vesicles, and transport from the synaptic cleft. Changes in these activities affect the pathogenesis of neuropsychiatric and neurological diseases, and dopaminergic system also has a role in peripheral neuroendocrine tumors (Eisenhofer 2001, Koopmans et al. 2009) and in pancreatic β-cells (Freeby et al. 2008). Various PET radiopharmaceuticals have been developed to

image these processes (reviewed by Volkow et al. 1996, Vernhoeff 1999, Cropley et al. 2006, Elsinga et al. 2006).

[^{18}F]FDOPA (Fig. 2.4., Firnau et al. 1973, Garnett et al. 1978, Firnau et al. 1986), a fluorinated analog of the DOPA, the intermediate product in dopamine synthesis, is widely used for imaging dopamine synthesis in the central nervous system (Kumakura and Cumming 2009). [β-^{11}C]-L-DOPA and 6-fluoro-[β-^{11}C]-L-DOPA (Fig. 2.4., Hartvig et al. 1992) have also been evaluated as dopamine synthesis tracers; the decarboxylation rate of [β-^{11}C]-L-DOPA was twice that of 6-fluoro-[β-^{11}C]-L-DOPA, but even the decarboxylation rate of [β-^{11}C]-L-DOPA was slow for PET (Hartvig et al. 1992). On the other hand, [^{18}F]FDOPA is a better substrate for catechol-*O*-methyltransferase (COMT) than [β-^{11}C]-L-DOPA. [β-^{11}C]-L-DOPA results in lower plasma levels of radioactive metabolite than [^{18}F]FDOPA (Kumakura and Cumming 2009). [β-^{11}C]-L-DOPA is recently used in a study of regional dopamine synthesis in schitzophrenia patients (Nozaki et al. 2009). However, complex radioenzymatic synthesis limits its clinical use.

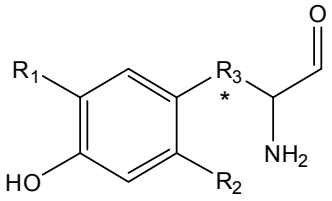

[^{18}F]FDOPA: R_1=OH, R_2=[^{18}F], R_3=CH_2
[^{18}F]FMT: R_1=H, R_2=[^{18}F], R_3=CH_2
[β-^{11}C]-L-DOPA: R_1=OH, R_2=H, R_3=[^{11}C]CH_2
6-fluoro-[β-^{11}C]-L-DOPA: R_1=OH, R_2=F, R_3=[^{11}C]CH_2

Figure 2.4. PET radiotracers for dopamine synthesis.

Of the fluorinated analogues of L-*m*-tyrosine, 6-[^{18}F]fluoro-L-*m*-tyrosine ([^{18}F]FMT, Fig. 2.4., Barrio et al. 1996) was found to be a suitable tracer for studying AADC activity, but it is not suitable for further investigation of the dopamine metabolic pathway (Doudet et al. 1999). Although the metabolic profile of [^{18}F]FMT is not as complicated as the metabolism of [^{18}F]FDOPA and is thus better for PET, relatively little has been published in terms of its brain uptake values, especially for normal human subjects (DeJesus 2003, Eberling et al. 2007).

To date, the majority of the interest in developing radiotracers for VMAT has focused on VMAT2. ^{11}C-labeled dihydrotetrabenazine ([^{11}C]DTBZ, Fig. 2.5.) was developed for imaging VMAT2 sites in monoaminergic neurons in the brain (Kilbourn et al. 1993), and currently it is also used for indirect measurement of pancreatic β-cell mass, which is known to be decreased in both diabetes mellitus types (Freeby et al. 2008).

An ^{18}F-labeled fluoroalkyl DTBZ derivative, [^{18}F]AV-133 (Fig. 2.5., Goswami et al. 2006, Okamura et al. 2010), was demonstrated to be an appropriate radiopharmaceutical

for mapping VMAT2 sites in rat and human brains, but optimization is still required for pancreatic β-cell labeling (Tsao et al. 2010). An ^{18}F-labeled epoxide dedivative of DTBZ exhibits selective binding to VMAT2 in the rat pancreas (Kung et al. 2008).

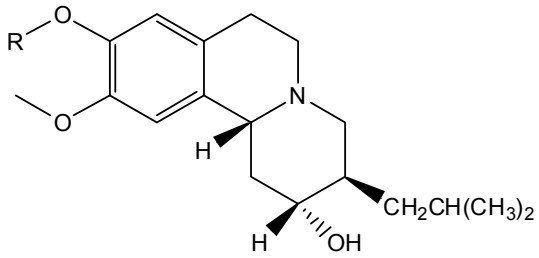

[^{11}C]DTBZ: R=[^{11}C]CH_3
[^{18}F]AV-133: R=[^{18}F]$CH_2CH_2CH_2$

Figure 2.5. PET radiotracers for VMAT2.

Many radiotracers of various chemical classes have been introduced to investigate the physiology and pharmacology of DAT (Laakso and Hietala 2000, Elsinga et al. 2006, Stehouwer and Goodman 2009). [^{11}C]Nomifensine (Fig. 2.6.) was one of the first tracers employed for *in vivo* imaging of DAT (Aquilonius et al. 1987). Other non-tropane tracers have also been developed, derived mainly from GBR 13119 (Kilbourn et al. 1992), but the largest amount of effort has been directed toward phenyltropane analogues of cocaine (Dollé et al. 2006, Stehouwer and Goodman 2009) such as 2β-carbomethoxy-3β-(4-fluorophenyl)tropane (β-CFT or WIN 35,428).

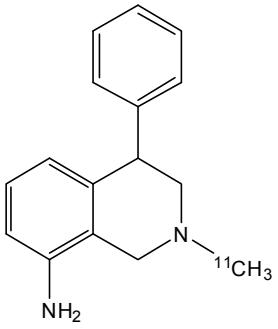

[^{11}C]Nomifensine

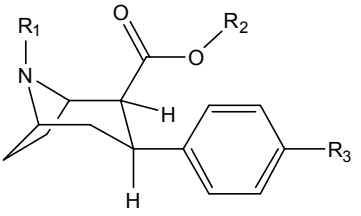

[^{18}F]CFT: R_1=R_2=CH_3, R_3=[^{18}F]
[^{11}C]CFT: R_1=[^{11}C]CH_3, R_2=CH_3, R_3=F
[^{18}F]FECNT: R_1=$CH_2CH_2{}^{18}F$, R_2=CH_3, R_3=Cl
[^{18}F]FECT: R_1= CH_3, R_2= $CH_2CH_2{}^{18}F$, R_3=Cl
[^{18}F]CFT-FE: R_1=$CH_2CH_2{}^{18}F$, R_2=CH_3, R_3=F
[^{18}F]CFT-FP: R_1=$CH_2CH_2CH_2{}^{18}F$, R_2=CH_3, R_3=F
[^{18}F]CIT-FP: R_1=$CH_2CH_2CH_2{}^{18}F$, R_2=CH_3, R_3=I
[^{18}F]FE-PE2I: R_1=CH_2CH=CHI, R_2=$CH_2CH_2{}^{18}F$, R_3=CH_3

Figure 2.6. PET radiotracers for DAT**.**

β-CFT labeled with ^{11}C (Fig. 2.6.) was found to be selective for DAT, but the half-life of ^{11}C was too short for the binding equilibrium (Wong et al. 1993). [^{18}F]CFT (Fig. 2.6., Haaparanta et al. 1996) has a longer ^{18}F half-life and is suitable for *in vivo* studies of DAT in humans (Laakso et al. 1998). Many other tropane analogues such as [^{18}F]FECNT (Goodman et al. 2000, Zoghbi et al. 2006), [^{18}F]FECT (Wilson et al. 1996, Chitneni et al. 2008), [^{18}F]CFT-FE (Harada et al. 2004), [^{18}F]CFT-FP (Kämäräinen et al. 2000, Koivula et al. 2008), and [^{18}F]CIT-FP (Ma et al. 2002) exhibit high or moderate affinity to other monoamine transporters, NET, and serotonin transporters (SERT), or undergo extensive metabolism. More recently, a new ^{18}F-labeled tropane analog, [^{18}F](E)-N-(3-iodoprop-2-enyl)-2β-carbofluoroethoxy-3β-(4'-methyl-phenyl) nortropane (Fig. 2.6., [^{18}F]FE-PE2I), was shown to be a promising radiotracer for DAT (Schou et al. 2009), but it is limited by its fast metabolism (Varrone et al. 2009).

2.4. [^{18}F]FDOPA, a dopamine synthesis tracer

[^{18}F]FDOPA was first reported as a PET tracer for pre-synaptic dopaminergic functions in 1983 (Garnett et al. 1983). Fluorination of DOPA results in three ring-fluorinated isomers, 2-, 5-, and 6-fluorodopa, all of which are substrates for COMT, but the rate constant of the metylation catalyzed by COMT significantly differs among these isomers. 6-fluorodopa exhibited the most suitable properties for *in vivo* imaging; 2- and 5-fluorodopa were metabolized three to four times faster than DOPA, while 6-fluorodopa displayed a slower metabolism than DOPA (Creveling and Kirk 1985). Striatal [^{18}F]FDOPA accumulation reflects the transport of [^{18}F]FDOPA into nigrostriatal nerve terminals, the activity of AADC, storage of [^{18}F]fluorodopamine ([^{18}F]FDA) within vesicles, and the number of functioning nerve terminals (Garnett et al. 1978, Firnau et al. 1987).

2.4.1. Metabolism of [^{18}F]FDOPA

The metabolism of [^{18}F]FDOPA is complex (Fig. 2.7). In the periphery, [^{18}F]FDOPA is converted into [^{18}F]FDA by AADC and into 3-*O*-methyl-6-[^{18}F]fluoro-L-DOPA (3-[^{18}F]OMFD) by COMT, and further converted to [^{18}F]FDA sulphate, 3,4dihydroxy-6-[^{18}F]fluorophenylacetic acid ([^{18}F]FDOPAC), and 6-[^{18}F]fluorohomovanillic acid ([^{18}F]FHVA) by monoamine oxidase (MAO) and by aldehyde dehydrogenase (AD) and to different sulphates ([^{18}F]FD-SO_4, [^{18}F]FDA-SO_4, [^{18}F]FDOPAL-SO_4, [^{18}F]FDOPAC-SO_4) by phenolsulfotransferase (PST). [^{18}F]FDOPA and 3-[^{18}F]OMFD can penetrate the blood-brain barrier, but only ~1% of the injected [^{18}F]FDOPA enters the brain, where it is metabolized to [^{18}F]FDA and stored in synaptic vesicles.

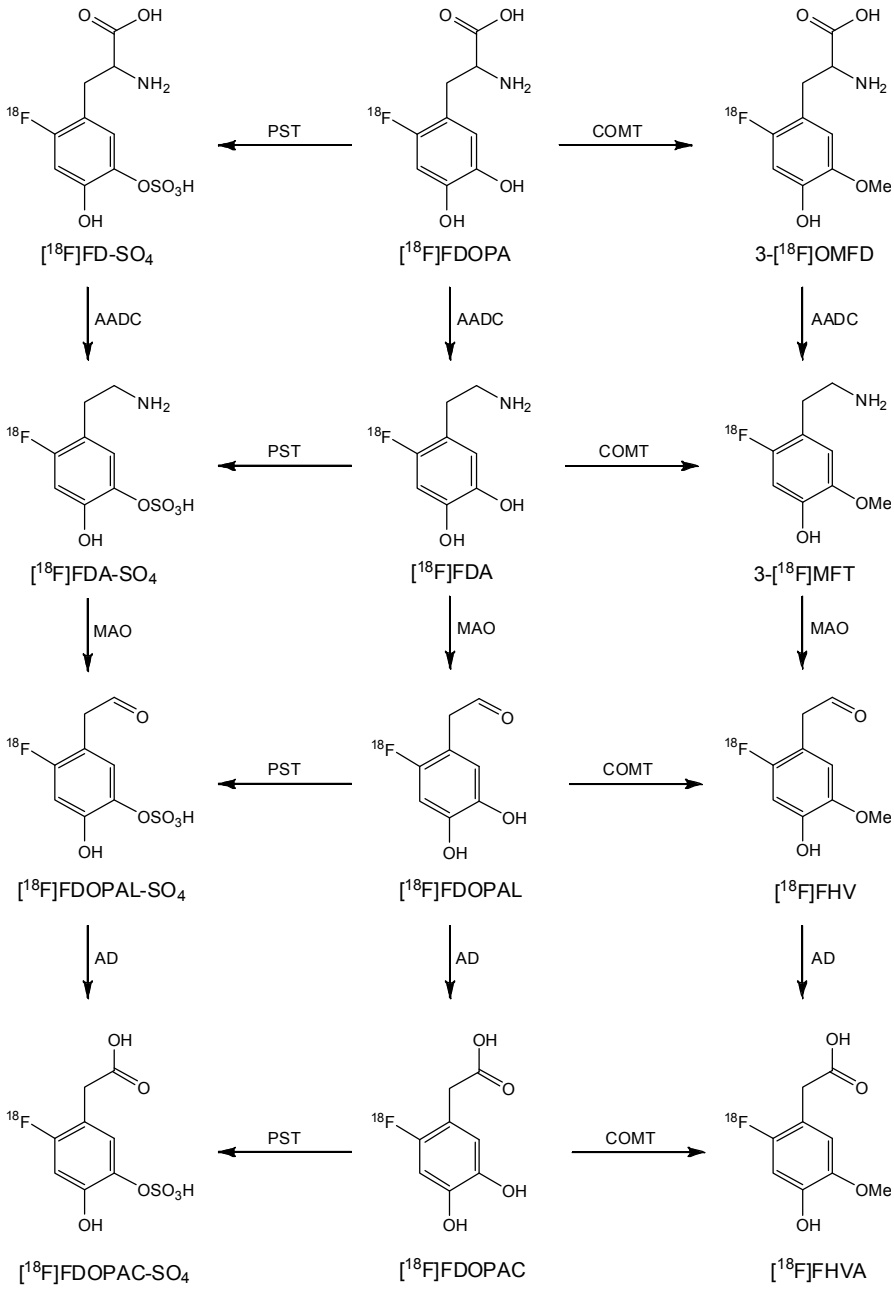

Figure 2.7. Main metabolism of [^{18}F]FDOPA.

When released from the vesicles, [^{18}F]FDA is metabolized to [^{18}F]FDOPAC, 3-methoxy-6-[^{18}F]fluorotyramine (3-[^{18}F]MFT), and [^{18}F]FHVA (Firnau et al. 1987, Melega et al. 1990). 3-[^{18}F]OMFD adopts an essentially uniform distribution in the brain, diminishing image contrast and complicating analysis. To minimize peripheral metabolism, COMT and AADC inhibitors can be used prior to [^{18}F]FDOPA injection (Hoffman et al. 1992, Ruottinen et al. 1995).

Despite its extensive metabolism, [^{18}F]FDOPA has been used for PET imaging mainly for evaluation of dopaminergic terminals in PD (Sioka et al. 2010). Other neuropsychiatric disorders such as mania, schizophrenia, autism, attention deficit hyperactivity disorders, and drug abuse have also been studied with [^{18}F]FDOPA and PET (DeJesus 2003). [^{18}F]FDOPA is increasingly implemented in the evaluation of hyperinsulinemia in infants and of neuroendocrine tumors (Becherer et al. 2004, Ribeiro et al. 2005, Minn et al. 2009).

2.4.2. Nucleophilic synthesis of [^{18}F]FDOPA

Direct nucleophilic replacement of a leaving group in the benzene ring is impossible without ring activation using an electron-withdrawing substituent. The nucleophilic NCA synthesis of [^{18}F]FDOPA therefore consists of several steps (Fig 2.8., Lemaire et al. 1990, Reddy et al. 1993). The first step of this route was displacement of the nitro group in 6-nitroverataldehyde **(1a)** or 6-nitropiperonal **(1b)** by [^{18}F]F$^-$. The resulting fluorinated aldehydes **(2a, 2b)** were purified via two C-18 Sep Pak cartridges. In the second step, aldehydes **(2a, 2b)** were coupled with 2-phenyl-5-oxazolone in the presence of 1,4-diazabicyclo[2,2,2]octane (DABCO) as a base. The third step included reductive hydrolysis of the azlactone derivative **(3)** and preparative purification to obtain a racemic mixture of the D- and L-isomers of ^{18}F-labeled DOPA **(4)**. The isomers were separated by chiral HPLC. The total synthesis time, including separations, was approximately two hours. The decay-corrected RCYs of [^{18}F]FDOPA were 3-5% (Reddy et al. 1993) or 10% (Lemaire et al. 1990), and the SA was 44 GBq/μmol (Lemaire et al. 1990). This method was regiospecific, producing only the 6-isomer, but not stereospecific; both D- and L-enantiomers were obtained in equal amounts, requiring chiral HPLC separation in a time- and yield-consuming step.

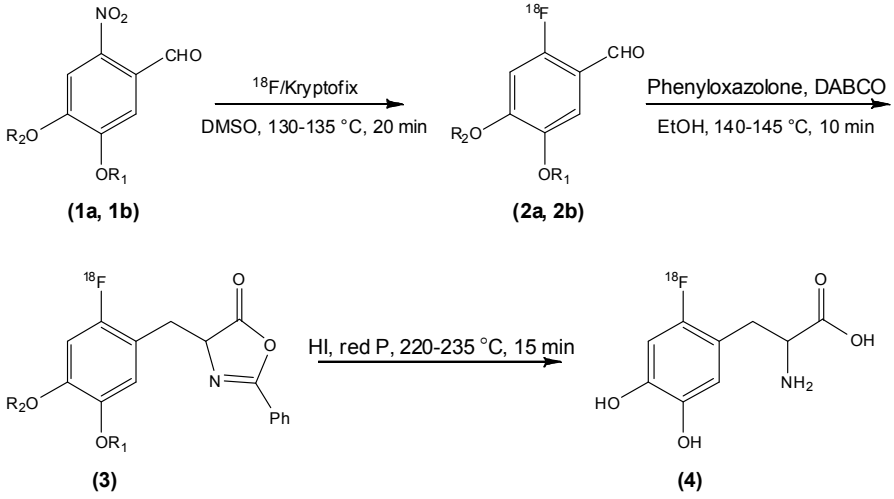

Figure 2.8. Nucleophilic synthesis of [^{18}F]FDOPA **(4)**.
(1a, 2a) R_1=R_2=CH_3; **(1b, 2b)** R_1,R_2= -CH_2-.

Various enantioselective approaches have been developed to improve the nucleophilic production of [^{18}F]FDOPA, several of which rely on the same precursors as in Fig. 2.8. (**1a, 1b**; Lemaire et al. 1991, 1993, Nafaji 1995). The fluorinated aldehydes (**2a, 2b**) were converted to the corresponding fluorobenzyl alcohols by $NaBH_4$, then to fluorobenzyl bromides by $SOBr_2$. A chiral substrate, (1R,2R,5R)-[(+)-2-hydroxypinanyl-3-idene]glycine t-butyl ester, was then alkylated by the fluorobenzyl bromides in the presence of a base. The synthesis time was 120 min and the decay-corrected RCY was 10%, but the enantiomeric purity was less than 75% in the L-form (Lemaire 1991).

This enantiomeric purity was improved by using the 1-(S)-(-)camphor imine of t-butyl glycinate or (S)-(-)-1-Boc-2-t-butyl-3-methyl-4-imidazolidinone ((S)-Boc-BMI) as a chiral substrate in the alkylation step (Lemaire et al. 1993), with final enantiomeric excesses of 83% and 96%, respectively. The synthesis time, 110 min, and decay-corrected RCY, 5-10%, were still insufficient for routine synthesis. The RCY was slightly improved through optimization to 6-13% (non-decay-corrected), and the synthesis time was shortened to 85 min (Nafaji 1995). By changing the precursor (**1a**) to trimethylammonium verataldehyde triflate and using fluorobenzyl iodide instead of fluorobenzyl bromide for alkylation of (S)-Boc-BMI, the decay-corrected RCY was increased to 23 ± 6% in a reasonable synthesis time of 90 min (Lemaire et al. 1994). This method was used in routine production with good radiochemical and enantiomeric purities (>97%), but automation was limited due to the alkylation reaction which required the strong base under anhydrous conditions.

To overcome this drawback, chiral phase-transfer catalyst (PTC) derived from a Cinchona alkaloid was used in the alkylation step (Yin et al. 2003, Lemaire et al. 2004); *O*-allyl-*N*-(9-anthracenylmethyl)cinchonidium catalyzed the enantioselective alkylation of the Schiff base *N*-(diphenylmethylene)glycine *tert*-butyl ester. The methylene group of the Schiff base was deprotonated by cesium hydroxide and alkylated by 2-[^{18}F]fluoro-4,5-dimethoxybenzyl iodine or bromide. After systematic optimization of the reaction conditions, [^{18}F]FDOPA was obtained in a 25-30% decay-corrected RCY with a synthesis time of 100 min (Lemaire et al. 2004). This method avoided low temperatures and chiral preparative separation, and the automated PTC-based synthesis device produced radiochemically and enantiomerically pure [^{18}F]FDOPA with 20 ± 4% RCY in 120 min and with a SA of 50 GBq/μmol (Shen et al. 2009).

Another PTC method utilized 2-amino-2'-hydroxy-1,1'-binaphtyl (*(S)*-NOBIN) and an achiral Ni(II) complex of a Schiff base of (*S*)-*O*-[(*N*-benzylpropyl)amino]benzophenone and glycine, (NiPBPGly), as a substrate/catalyst pair (Krasikova et al. 2004). The alkylation of NiPBPGly with 3,4-methylendioxy-6-[^{18}F]fluorobenzyl bromide occurred at room temperature, with a synthesis time of approximately 120 min and an [^{18}F]FDOPA RCY of 16 ± 5%. The RCP was >99% and enaniomerical purity >96%.

3,4-methylendioxy-6-[^{18}F]fluorobenzyl bromide was also used as an alkylating agent in asymmetric alkylation of the chiral Ni(II) complex (Krasikova et al. 2007). Complexes containing various substituents in the benzyl group were tested in the production of [^{18}F]FDOPA. The Ni(II) complex derived from *(S)-N*-(2-benzoylphenyl)-1-(3,4-dichlorobenzyl)pyrrolidine-2-carboxamide yielded the highest enantiomeric purity, and the alkylation was performed under mild conditions appropriate for automation of the synthesis. The decay-corrected RCY was 10-15% with a synthesis time of 120 min, and the RCP and chemical purity exceeded 99%.

Enzymatic reactions occur under mild conditions with high efficiency and selectivity. The enzymatic synthesis of NCA [^{18}F]FDOPA using β-tyrosinase generated radiochemically and enantiomerically pure final product (Kaneko et al. 1999). The RCY was low based on the initial amount of [^{18}F]F$^-$, 2% decay-corrected, and the synthesis time was 150 min. Thus, this method did not improve [^{18}F]FDOPA synthesis compared to previously described syntheses.

In order to simplifie the multi-step nucleophilic production methods of [^{18}F]FDOPA, a direct nucleophilic isotopic exchange reaction on a formyl-activated protected aromatic amino acid derivative was studied (Wagner et al. 2009). Baeyer-Villiger oxidation of the formyl group and subsequent acid hydrolysis followed the ^{19}F/^{18}F exchange in a one-pot reaction. After optimization of these three steps, the RCY was 22 % in a synthesis time of 105 min. The enantiomeric purity exceeded 96 %. This method suffers from the low SA because of the fluoride in the precursor: the SA was reported to approximately five-fold higher than the SA of 0.3 GBq/μmol achieved using electrophilic radiofluorination.

2.4.3. Electrophilic synthesis of [^{18}F]FDOPA

The first electrophilic method for production of [^{18}F]FDOPA utilized 3-*O*-methyl-L-DOPA ethyl ester as a precursor (Firnau et al. 1980). This precursor was labeled with [^{18}F]XeF_2 in hydrogen fluoride (HF) and the resulting product was hydrolyzed to [^{18}F]FDOPA with hydrobromic acid (HBr). The [^{18}F]FDOPA employed in the first human PET studies was produced with this method (Garnett et al. 1983). However, the ^{18}F/^{19}F-exchange between [^{18}F]XeF_2 and HF lowered the RCY to less than 1% at the end of synthesis (EOS, Firnau et al. 1984).

[^{18}F]CH_3COOF in glacial acetic acid proved to be a more reactive labeling agent than [^{18}F]XeF_2. This synthesis route produced all possible structural isomers: 2-[^{18}F]fluoro-L-DOPA, 5-[^{18}F]fluoro-L-DOPA, and [^{18}F]FDOPA (Chirakal et al. 1984b). Thus, the RCY of [^{18}F]FDOPA was only 1.3% at EOS.

The direct ^{18}F-fluorination of L-DOPA using [^{18}F]F_2 in HF with (Chirakal et al. 1986) or without (Firnau et al. 1984) boron trifluoride (BF_3) was studied in order to improve the RCY of [^{18}F]FDOPA. [^{18}F]F_2 (180-190 μmol) was diluted with 0.5% F_2 in neon and passed through the precursor (430-470 μmol) at -65 ºC. These approaches

including or excluding BF_3 provided a mixture of 2-[^{18}F]fluoro-L-DOPA, 5-[^{18}F]fluoro-L-DOPA, and [^{18}F]FDOPA. Following investigation of the substitution of HF with acetonitrile or water and the use of *O*-methyl derivatives of L-DOPA as the precursor, it became clear that while the addition of BF_3 to the reaction mixture improved the RCY of [^{18}F]FDOPA, HF could not be replaced without loss in the RCY, with the hydrolysis of *O*-methyl lowering the RCY (Chirakal et al. 1986). The RCY after two hours of synthesis was 9% and the SA was 0.008 GBq/µmol. Chemical and RCP exceeded 97%. Comparison of the reactivity and selectivity of [^{18}F]F_2 and [^{18}F]CH_3COOF in the direct electrophilic labeling of aromatic amino acids in various solvents revealed that the RCY favored the use of trifluoroacetic acid as a solvent. However, the 2-isomer was prominent in the labeling of L-DOPA (Coenen et al. 1988).

Various protected derivatives of L-DOPA as precursors in electrophilic labeling were studied to improve regioselectivity (Chaly and Diksic 1986, Adam et al. 1986a, 1986b). L-DOPA protected by phosgene improved the RCY to 21 ± 4% at EOS; the synthesis time was 50 min, the RCP was 95 ± 2%, and the SA was 0.028 GBq/µmol (Chaly and Diksic 1986). [^{18}F]CH_3COOF as a labeling agent produced only small amounts of 5-[^{18}F]fluoro-L-DOPA in addition to [^{18}F]FDOPA. Although more reactive, [^{18}F]F_2 was less regioselective. However, phosgene is hazardous, and the phosgene derivative of L-DOPA was very sensitive to moisture. The effects of various protecting groups on fluorine incorporation into the aromatic ring were assessed by labeling 12 different L-DOPA derivatives with [^{18}F]CH_3COOF in glacial acetic acid (Adam et al. 1986a). The highest RCY was obtained with L-methyl-N-acetyl-[β-(methoxy-4-acetoxyphenyl)]alanine, and the protecting groups were removed by hydrolysis with hydrogen iodide. The RCY at the end of bombardment (EOB) ranged from 5.1 to 10.7%. 2-isomer was obtained with approximately the same RCY as [^{18}F]FDOPA (Adam et al. 1986b).

The enantiomeric purity achieved with the above methods was >95% in the L-form due to the use of chiral precursors. Regioselectivity of the electrophilic fluorination was more difficult to achieve, prompting the introduction of radiofluorodemetalation. The first attempt was the fluorodesilylation of 6-trimethylsilyl-3,4-dimethoxy-L-DOPA ethyl ester (200 µmol) in carbon tetrachloride/Freon using 70 µmol [^{18}F]F_2 (Diksic and Farrokhzad 1985). Protecting groups were removed by acidic hydrolysis with 48% HBr. This method generated only the desired 6-isomer, simplifying the purification of the final product and reducing the synthesis time to less than one hour. The RCY was 8% at EOS and the SA was 0.025 GBq/µmol. However, the preparation of the precursor was difficult, making this method unattractive for routine production of [^{18}F]FDOPA.

The preparation of the precursors for fluorodemercuration, for example N-(trifluoroacetyl)-3,4-methoxy-6-trifluoroacetoxy-mercurio-L-phenylalanine ethyl ester (Luxen et al. 1990) or L-methyl-N-acetyl-[β-(3,4-dimethoxy-6-mercuric-trifluoroacetyl-phenyl)]alanine (Adam and Jivan 1988), was more straightforward than

the preparation of the silyl precursor. The use of chloroform stabilized with ethanol as a solvent in the fluorodemercuration reaction with [^{18}F]CH_3COOF provided a decay-corrected RCY of 12%, and chloroform stabilized with isopentene as a solvent in the fluorination reaction resulted in the loss of approximately half of the RCY (Adam and Jivan 1988). Luxen et al. (Luxen et al. 1990) used chloroform or a mixture of chloroform and Freon in the fluorination step, even though the best RCY was achieved using acetic acid, because lower boiling points made chloroform and Freon more convenient for routine production of [^{18}F]FDOPA. [^{18}F]F_2 was too reactive, resulting in a complex reaction mixture, while [^{18}F]CH_3COOF generated fewer byproducts with a RCY of 11% (Luxen et al. 1990). However, due to the high toxicity of mercury, both methods required careful removal of excess mercury and mercurated products prior to the final HPLC purification of [^{18}F]FDOPA. Mercury removal was avoided by developing an insoluble polymer-bound protected mercurated [^{18}F]FDOPA precursor (Szajek et al. 1998); these modified polystyrene supports were convenient for automated [^{18}F]FDOPA production. The decay-corrected RCY was 6.6% after one hour of synthesis and the SA exceeded 0.024 GBq/µmol.

Luxen et al. reviewed [^{18}F]FDOPA production methods based on non-regioselective electrophilic fluorination, regioselective fluorodemetalation, or nucleophilic substitution methods developed prior to 1992 (Luxen et al. 1992). They recommended either direct fluorination of the fully protected precursor (Adam et al. 1986a,b) or regioselective fluorodemercuration (Adam and Jivan 1988, Luxen et al. 1990) for routine [^{18}F]FDOPA production. Nucleophilic labeling using (S)-Boc-BMI had been introduced by 1992, but the optimization of the method in terms of synthesis time and RCY was still under investigation (Lemaire et al. 1993). Regioselective radiofluorodestannylation for [^{18}F]FDOPA production (Fig. 2.9, Namavari et al. 1992) was introduced during the same time period.

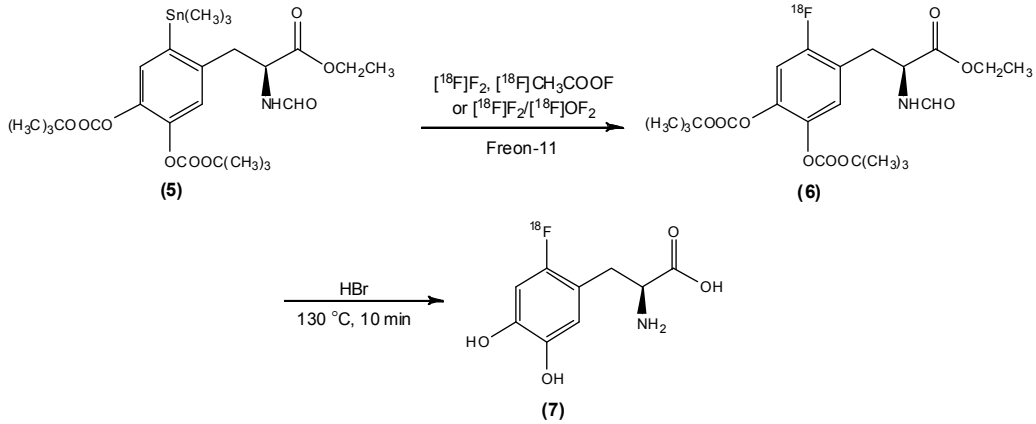

Figure 2.9. Regioselective fluorodestannylation for production of [^{18}F]FDOPA **(7)**.

[^{18}F]F_2, [^{18}F]CH_3COOF, or a mixture of [^{18}F]F_2 and oxygen [^{18}F]difluoride ([^{18}F]OF_2) (100 µmol each) was used as a labeling agent in the fluorodestannylation of 101 µmol N-formyl-3,4-di-*t*-butoxycarbonyloxy-6-(trimethylstannyl)-L-phenylalanine ethyl ester **(5)** in trichlorofluoromethane (Freon-11). The protected intermediate **(6)** was purified before removal of the protecting groups. The decay-corrected RCY with [^{18}F]CH_3COOF was significantly lower than with [^{18}F]F_2 or the mixture of [^{18}F]F_2 and [^{18}F]OF_2 (8%, 25%, and 23%, respectively). The *tert*-butoxy groups were chosen to protect the hydroxyl groups as they facilitate fluorodestannylation and can be easily removed via acidic hydrolysis with HBr.

Direct electrophilic fluorination of 4-*O*-pivaloyl-L-DOPA or 3,4-di-*O*-pivaloyl-L-DOPA in acetic acid was also investigated (Ishiwata et al. 1993), revealing that the pivaloyl groups were easily removed by HCl hydrolysis without racemization. However, the requirement for fluorination regioselectivity was not satisfied; 2,6-difluorodopa and the 2- and 5-isomers of FDOPA were present in the reaction mixture (Hatano et al. 1996). This investigation also introduced a preparative purification method based on the use of physiological saline containing ascorbic acid and ethylenediaminetetraacetic acid as an eluent, a solution that can be administered to humans directly after sterile filtration.

At present, regioselective radiofluorodestannylation (Namavari et al. 1992) is the most common electrophilic route for generating [^{18}F]FDOPA (Table 2.3). Dollé and co-workers (Dollé et al. 1998) improved Namavari's method by using a new fully protected stannylated precursor, *N*-(*tert*-butoxycarbonyl)-3,4-di(*tert*-butoxycarbonyloxy)-6-trimethylstannyl-L-phenylalanine ethyl ester. The decay-corrected RCY of [^{18}F]FDOPA after 45-50 min synthesis was 26%, with a SA of 0.004 GBq/µmol. Precursor synthesis was further improved by Füchtner (Füchtner et al. 2002), and de Vries et al. developed a fully automated synthesis module based on radiofluorodestannylation, abandoning the purification of the protected intermediate (de Vries et al. 1999). These modifications led to no significant change in the purity or the SA of the final product, while the RCY was increased to 33% and the SA was 0.01 GBq/µmol. de Vries et al. also tested chloroform and acetonitrile as alternative solvents for the fluorination reaction, due to the ozone layer-depleting properties of Freon-11. However, a radical loss (61-73%) of radioactivity occurred during the evaporation of chloroform or acetonitrile after the labeling reaction, a loss that did not occur when using Freon-11 as a solvent.

A commercial synthesis module based on fluorodestannylation (TRACERlab FX_{FDOPA}, GE Healthcare, Chalfont St. Giles, UK) offers [^{18}F]FDOPA with an RCY of 20% in 55 min, including synthesis preparation time. This module was used in a study aiming to replace Freon-11 with chloroform in which three types of chloroform with different stabilizers were tested (Füchtner et al. 2008). Chloroform was evaporated prior to hydrolysis by heating the reaction mixture to 80 °C under vacuum for 5 min. Deuterochloroform stabilized with silver was the only stabilizer that resulted in no

significant loss of radioactivity during the evaporation. [^{18}F]FDOPA appropriate for human studies was produced with a RCY of 25 ± 3% (Füchtner et al. 2008). Also a similar module, TRACERLab Fx-FE (GE Healthcare) with the synthesis procedure similar to de Vries (de Vries et al. 1999), was applied to good manufacturing practice production of [^{18}F]FDOPA that fulfills United States Pharmacopoeia requirements (Kao et al. 2011).

Table 2.3. Selected reaction conditions and outcomes for fluorodestannylation.

	Namavari et al. 1992	**Dollé et al. 1997**	**de Vries et al. 1999**	**Kao et al. 2011**
Fluorination reagent	[^{18}F]F_2, [^{18}F]OF_2/[^{18}F]F_2 or [^{18}F]CH_3COOF	[^{18}F]F_2	[^{18}F]F_2	[^{18}F]F_2
F_2-carrier [µmol]	100	n.m.	95 ± 15	n.m.
Precursor [µmol]	101	180	97	97
Freon-11 [ml]	10	20	10	10
Protected intermediate	Purified	Purified	Not purified	Not purified
Deprotection (48% HBr)	2 ml 130°C, 10 min	2 ml, 130°C, 10 min	2 ml, 130°C, 10 min	n.m. 130°C, 10 min
Yield [MBq]	3145	850–1000	556 ± 125	2600 ± 260
RCY [%]	25 (with [^{18}F]F_2)	26	33 ± 4	39.8 ± 3.9
SA [GBq/µmol]	n.m.	0.004	0.01 ± 0.002	0.04 ± 0.003
Synthesis time [min]	60	45-50	45	> 40

n.m. not mentioned

2.5. [^{18}F]CFT, a dopaminetransporter tracer

2.5.1. CFT

2-β-carbomethoxy-3-β-(4-fluorophenyl)tropane (CFT, Win 35,428) is a fluorinated cocaine analog lacking an ester group between the tropane and phenyl rings (Clarke et al. 1973). The lack of the ester moiety between these moieties enhances the stimulant activity of the molecule versus cocaine, and substitution of the para-hydrogen of the benzene ring with fluoride improves the activity even further (Clarke et al. 1973). CFT crosses the blood-brain barrier, exhibits similar inhibition potencies toward DAT, NET, and SERT *in vitro*, and is a potent nervous system stimulant

(Heikkila et al. 1979). A high density of [^{3}H]CFT binding was detected *in vitro* in the primate striatum and nucleus accumbens (Canfield et al. 1990, Kaufman et al. 1991). It became clear that [^{3}H]CFT accumulated in dopaminergic nerve terminals; *in vivo* studies in the mouse brain revealed that the highest uptake occurred in the striatum. There was no specific uptake in the cerebellum, allowing this region to be used as reference for non-specific binding. The uptake was demonstrated to peak after 30-60 min, and the ratio of specific to non-specific binding (striatum-cerebellum ratio) was ~2.5 (Scheffel et al. 1991). Drug competition studies indicated that the *in vivo* accumulation of [^{3}H]CFT in mice was inhibited by compounds with high affinity to DAT such as GBR 12909, and 50% occupation of receptors in mice occurred at a dose of 0.24 μmol/kg (Scheffel et al. 1991). Despite the high inhibition potency of CFT toward SERT, there was no *in vivo* accumulation of [^{3}H]CFT to SERT-rich areas (Scheffel et al. 1991). Similar results were observed in monkey *in vitro* studies; there was little or no [^{3}H]CFT binding in regions that contained significant densities of NET or SERT sites (Kaufman et al. 1991). However, in an *ex vivo* monkey study, moderate uptake of [^{3}H]CFT also occurred in the LC, a brain area with high NET density (Kaufman and Madras 1992). In the same study, a striatum-to-cerebellum ratio of 5.6 was achieved 90 min after [^{3}H]CFT administration (Kaufman and Madras 1992). Since significantly lower [^{3}H]CFT uptake was observed in brain sections of PD patients than in a human postmortem control sections, the possibility emerged of using radiolabeled CFT derivatives for single-photon emission computerized tomography (SPECT) or as PET imaging probes for presynaptic dopaminergic nerve terminals (Kaufman and Mardas 1991).

2.5.2. Halogenated analogues of CFT

Following the discovery that the addition of fluoride to a cocaine analog enhanced its activity (Clarke et al. 1973), the use of halogens other than fluorine expanded. The iodo analog 2-β-carbomethoxy-3-β-(4-[^{123}I]iodophenyl)tropane ([^{123}I]CIT, Neumeyer et al. 1991) was found to be a promising SPECT ligand for imaging DAT in humans (Kuikka et al. 1993). CIT exhibited an even higher affinity to DAT than CFT, but it also displayed a high affinity to SERT (Neumeyer et al. 1991). Binding profiles of CIT and other halogenated analogues of CFT to DAT and SERT appear in Table 2.4.

Table 2.4. Binding profiles of CFT and it's other halogenated analogues to DAT and SERT (inhibition of [^{3}H]CFT and [^{3}H]citalopram binding, respectively, in Cynomolgus Monkey striatum). All values are half maximal inhibitory concentrations (IC_{50}), nM (Melzer et al. 1993).

	DAT [IC_{50}, nM]	**SERT [IC_{50}, nM]**
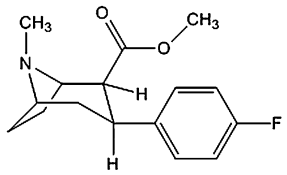	11 ± 1.0	160 ± 20
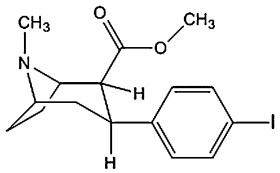	1.1 ± 0.06	2.5 ± 0.02
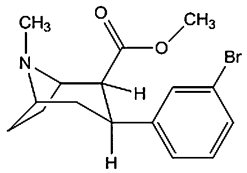	8.0 ± 0.08	20.4 ± 1.1
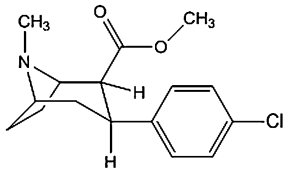	1.4 ± 0.04	5.9 ± 2.8

CIT has also been labeled with ^{11}C (Müller et al. 1993). In human studies, the striatum-to-cerebellum ratio was approximately two 60 min after of [^{11}C]CIT injection, at which time the uptake to the striatum was still increasing, and the uptake did not reach equilibrium within the time limit of the PET study (Farde et al. 1994). In addition to the high SERT affinity and slow kinetics, another drawback of radiolabeled CIT analogues is the formation of a lipophilic metabolite that can interfere with DAT quantitation (Bergström et al. 1995).

The bromo analog 2-β-carbomethoxy-3-β-(4-[^{76}Br]bromophenyl)tropane ([^{76}Br]CBT) was also investigated (Maziere et al. 1995). *In vitro* competition and saturation pharmacological assays showed that [^{76}Br]CBT primarily labeled DAT (Loc'h et al. 1995). In rats, a striatum-to-cerebellum ratio of 17 was measured 24 hours after the injection of [^{76}Br]CBT (Loc'h et al. 1995). Use of the chlorinated analog [*N*-^{11}C]2-β-carbomethoxy-3-β-(4-chlorophenyl)tropane ([^{11}C]RTI-31, Meltzer et al. 1993, Wilson et al. 1996) led to a striatum-to-cerebellum ratio of 4 in cynomolgus monkeys 90 min after the injection of [^{11}C]RTI-31 (Meltzer et al. 1993). These analogues displayed

equal affinities to SERT compared to DAT (Table 2.4, Meltzer et al. 1993). To date, no human studies employing either [^{76}Br]CBT or [^{11}C]RTI-31 have been reported.

2.5.3. [^{11}C]CFT

The N-methyl group in the tropane moiety of CFT enables straightforward incorporation of ^{11}C into CFT via [^{11}C]methyl iodide (Dannals et al. 1993, Meltzer et al. 1993). [^{11}C]methyl triflate has also been used as a labeling agent in the production of [^{11}C]CFT (Någren et al. 1995). The highest uptake after [^{11}C]CFT injection was detected in the striatum in *in vivo* primate studies, with specific-to-nonspecific uptake ratios of five at 90 min after injection and 2.5-3 at 120 min after injection (Melzer et al. 1993, Wong et al.1993, respectively). Striatum uptake was lower in 1-methyl-4-phenyl-1,2,3,6-tetrahydropyridine (MPTP, a selective neurotoxin for striatal dopaminergic nerve terminals that contain transporters)-treated primates (Hantraye et al. 1992, Wong et al. 1993). In healthy humans, the striatum-to-cerebellum ratio was approximately five at 90 min after the [^{11}C]CFT injection, and no pharmacological effects were observed with an injected mass of 3.3 ± 2.3 μg (Wong et al. 1993). The amount of unmetabolized [^{11}C]CFT was ~70% when measured 80 min post-injection. In a study in patients with mild PD, reduction in the radioactivity uptake after [^{11}C]CFT injection was observed in the striatum and in the SN (Frost et al. 1993). [^{11}C]CFT has been used to image DAT in humans despite the observation that binding equilibrium is not achievable during a PET study due to the short half-life of ^{11}C. If the binding equilibrium is not reached with ^{11}C-labeled tracers in 60-90 min and with ^{18}F-labeled tracers in 5-6 hours, the PET image may be affected by regional blood flow (Laakso and Hietala 2000, Volkow et al. 1996). More recently, the ^{11}C label has been introduced into the *O*-methyl position, resulting in a shorter and simpler method for producing ^{11}C-labeled CFT (Yoder et al. 2009). Preliminary studies suggest that this *O*-methyl analog is quantitatively equivalent to the *N*-labeled analog in the rat striatum (Yoder et al. 2009).

2.5.4. [^{18}F]CFT

The unreachable binding equilibrium in [^{11}C]CFT studies and the presence of fluorine in the original structure of CFT motivated the development of a method to produce [^{18}F]CFT. [^{18}F]CFT was synthesized by electrophilic fluorodestannylation using [^{18}F]CH_3COOF as a labeling agent (Haaparanta et al. 1996, Bergman et al. Finnish Patent 96603). This route utilized post-target-produced [^{18}F]F_2, which is the only means to generate electrophilic labeling agent with a SA sufficient for [^{18}F]CFT synthesis for clinical use. The decay-corrected RCY calculated from [^{18}F]F^- was 0.9-2%, and the SA was 11-16 GBq/μmol. *Ex vivo* rat studies demonstrated that the highest radioactivity accumulation in the brain occurred in the striatum, while in the periphery, the highest level of radioactivity was detected in the liver. Radioactivity uptake values were also relatively high in the kidney, spleen, and lung, and uptake to these organs

increased for 30 min after [^{18}F]CFT injection, decreasing thereafter. The striatum-to-cerebellum ratio peaked at 9.6 ± 0.7 120 min after injection (Haaparanta et al. 1996), a measurement in good agreement with a recent study in which the ratio was 9.2 ± 2.0 at 120 min after injection (Marjamäki et al. 2009). The same study reported NET-specific uptake of radioactivity in the rat LC. [^{18}F]CFT has been reported to be relatively resistant to metabolism; in a microdialysis study lasting 120 min in rodents, the amount of unmetabolized [^{18}F]CFT was ~64% of the total ^{18}F radioactivity (Haaparanta et al. 2004).

The suitability of [^{18}F]CFT as a radioligand for *in vivo* studies of DAT in humans has been evaluated (Laakso et al. 1998), and [^{18}F]CFT has been used in human studies of PD (Rinne et al. 1999a, Rinne et al. 1999b, Nurmi et al. 2000a, Nurmi et al. 2000b, Rinne et al. 2001, Nurmi et al. 2003), schizophrenia (Laakso et al. 2000a, Laakso et al. 2001), and detached personality (Laakso et al. 2000b). The SA achieved by the electrophilic method was sufficient for human studies, and the injected amount of cold CFT was ~4 μg in all of the preceding studies, an amount that was well tolerated by human subjects (Wong et al. 1993, Laakso et al. 1998). The kinetics of [^{18}F]CFT was relatively slow, but the half-life of ^{18}F allowed equilibrium between specific and nonspecific binding approximately four hours after administration in humans. In addition, a high target-to-non-target ratio and a low metabolism make [^{18}F]CFT a suitable radiotracer for imaging DAT in humans using PET (Laakso et al. 1998). The high target-to-non-target ratio permits even the visualization of the SN in humans (Laakso et al. 1998).

2.6. Dopamine hypofunction measurement with ^{11}C- and ^{18}F-labeled tracers

[^{18}F]FDOPA and [^{18}F]CFT respond to different aspects of the presynaptic dopaminergic system; [^{18}F]FDOPA reflects the synthesis of [^{18}F]FDA and its storage, while [^{18}F]CFT is related to DAT. Both markers are sufficiently sensitive to detect dopaminergic hypofunction (dimished function of the dopaminergic system in early PD). The decline of [^{18}F]CFT uptake in PD patients compared to healthy controls was slightly greater than the decline of [^{18}F]FDOPA uptake (Rinne et al. 2001). This effect also emerged when comparing the uptake of a VMAT2 tracer [^{11}C]DTBZ, and [^{18}F]FDOPA; [^{18}F]FDOPA uptake was reduced less than the uptake of [^{11}C]DTBZ (Lee et al. 2000). These differences may be due to compensatory mechanisms that have been suggested to occur in PD. In theory, DAT sites are downregulated and thus the re-uptake of dopamine is decreased, leading to an increased dopamine concentration (Lee et al. 2000). DAT tracers such as [^{18}F]CFT or VMAT2 tracers such as [^{11}C]DTBZ consequently overestimate the dopaminergic hypofunction, while dopamine synthesis tracers such as[^{18}F]FDOPA underestimate it. In a study of age-related changes in the striatal dopaminergic system in monkeys, the reduction in the dopamine synthesis rate measured with [β-^{11}C]-L-DOPA was somewhat smaller than the reduction determined

using [^{11}C]CFT (Harada et al. 2002). In contrast, no between-tracer differences emerged when comparing the uptakes of [^{18}F]FDOPA and [^{11}C]N-(3-iodoprop-2-enyl)-2-beta-carbomethoxy-3-beta-(4-methylphenyl)nortropane ([^{11}C]PE2I) in MPTP-treated monkeys (Poyot et al. 2001). However, in this case the loss of dopaminergic processes was larger than in the above studies of humans with early PD.

3. AIMS OF THE STUDY

The aim of this study was to develop the electrophilic labeling synthesis of [^{18}F]FDOPA and [^{18}F]CFT for imaging different aspects of the presynaptic dopaminergic system *in vivo* with PET. The pharmacokinetics of [^{18}F]CFT and its specifity to monoamine transporters were also determined. Furthermore, the behaviors of [^{18}F]CFT and [^{18}F]FDOPA in an animal model of PD were compared.

The following goals were set:

1. to further develop the electrophilic fluorodestannylation method to generate [^{18}F]FDOPA with moderately high SA for clinical use, using post-target-produced [^{18}F]F_2 as a labeling agent

2. to investigate the use of chloroform, dichloromethane, acetone, and their deuterated analogues as solvents for electrophilic radiofluorination reactions for the synthesis of [^{18}F]FDOPA using post-target produced [^{18}F]F_2 from [^{18}F]F^-

3. to study the effect of acetic acid in the electrophilic fluorodestannylation production of [^{18}F]FDOPA

4. to perform electrophilic synthesis of [^{18}F]CFT with high SA, and to develop quality assurance for clinical PET studies

5. to determine the pharmacological specificity and selectivity of [^{18}F]CFT for monoamine transporters

6. to determine the human radiation dose from injection of [^{18}F]CFT, extrapolating the dose from the animal data using the OLINDA/EX 1.0 software

7. to compare the difference in the uptake of [^{18}F]FDOPA and [^{18}F]CFT in relation to dopaminergic function, and to assess their ability to reflect the degree of nigral neuronal loss in rats with unilaterally destroyed dopamine pathways in the midbrain

4. MATERIALS AND METHODS

4.1. Production of radiopharmaceuticals

4.1.1. Production of [^{18}F]F$^-$

[^{18}F]F$^-$ was obtained using the nuclear reaction ^{18}O(p,n)^{18}F by irradiating 700 µl ^{18}O-enriched water with a 17-MeV proton beam produced with an MGC-20 cyclotron (Efremov Institute of Electrophysical Apparatuses, St. Petersburg, Russia).

4.1.2. Production of [^{18}F]F_2 with high SA

[^{18}F]F_2 was synthesized in an electrical discharge chamber by ^{18}F/^{19}F exchange using an automated device that was controlled using a touch screen (Fig. 4.1). The ^{18}F source was NCA [^{18}F]fluoromethane, which was mixed with 1 µmol of carrier fluorine in neon (Ne/0.5 % F_2) inside the discharge chamber for the synthesis of [^{18}F]FDOPA and 0.29-0.4 µmol for the synthesis of [^{18}F]CFT. [^{18}F]fluoromethane was produced from methyliodide by a nucleophilic substitution reaction with [^{18}F]F$^-$/Kryptofix K2.2.2-complex in acetonitrile. A detailed description of [^{18}F]F_2 synthesis is presented elsewhere (Bergman and Solin 1997).

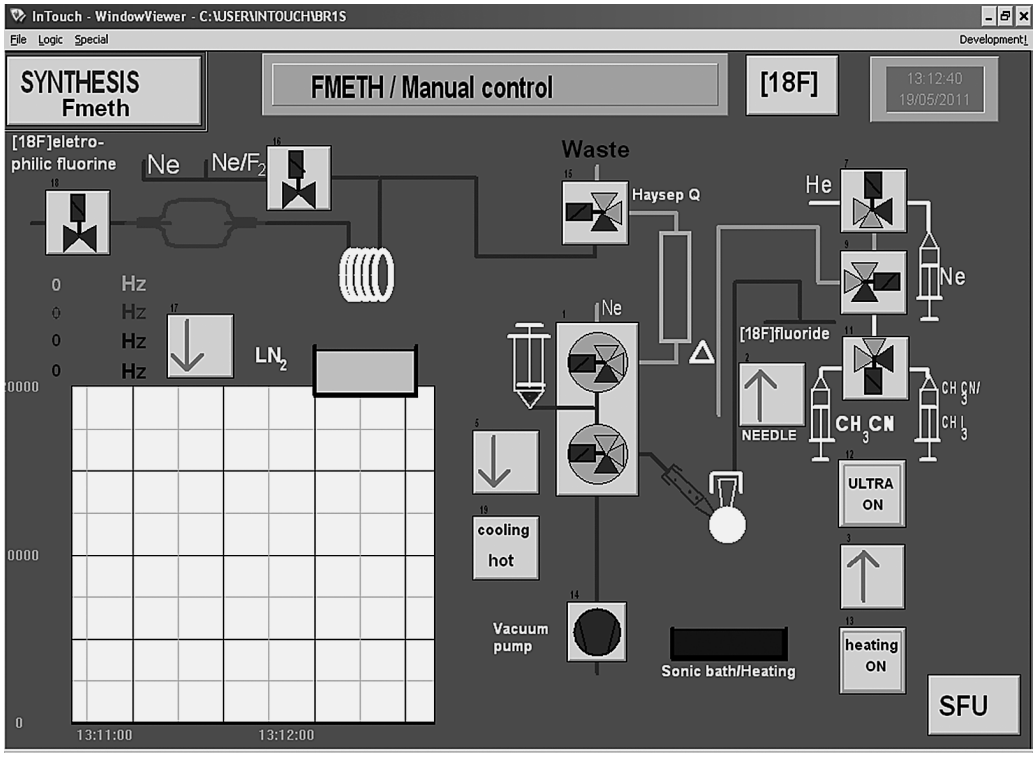

Figure 4.1. A touch-screen user interface for [^{18}F]F_2 production.

4.1.3. Synthesis of [^{18}F]FDOPA (I,II,IV)

The stannylated precursor (**5,** Fig. 5.1.) 4,5-di-[(1,1-dimethylethoxycarbonyl)oxy]-*N*-formyl-2-trimethylstannyl-L-phenylalanine ethyl ester (3.4-4.1 μmol in studies I and IV; 5 μmol in study II) was dissolved in a mixture of 700 μl Freon-11 plus acetic acid (25 μl, 430 μmol, studies I and IV). In study II, the precursor was dissolved in 700-750 μl of one of the following solvents: Freon-11 (CCl_3F), deuterated chloroform ($CDCl_3$), deuterated dichloromethane (CD_2Cl_2), deuterated acetone (C_3D_6O), chloroform ($CHCl_3$) stabilized with amylene, dichloromethane (CH_2Cl_2) stabilized with amylene, or acetone (C_3H_6O), and 0, 25, or 50 μl (0, 430, or 860 μmol) dry acetic acid. Solvents were added to the precursor solution prior to the labeling reaction, and [^{18}F]F_2 was bubbled through this mixture at room temperature. Freon-11 was evaporated using neon flow at room temperature. Other solvents were evaporated using neon flow and by heating the reaction vessel in an oil bath (40-60 °C). HBr (48%, 300 μl) was added to the residue to remove protecting groups. Hydrolysis was carried out at 130 °C for 5 min, and the reaction mixture was then partially neutralized by addition of 10.8 M NaOH (100 μl) and HPLC eluent (300 μl).

The resulting [^{18}F]FDOPA was purified by semi-preparative HPLC with a μBondapak C18 column (Waters Corp., Milford, MA, USA). A UV absorption detector at λ=280 nm and a 2 x 2-inch NaI(Tl) crystal for radioactivity detection were used. The column was eluted with 0.9% NaCl containing 0.01% acetic acid. The fraction containing the [^{18}F]FDOPA was collected, and for final formulation, this fraction was filtered through a sterile filter.

4.1.4. Synthesis of [^{18}F]CFT (III, IV)

The stannylated precursor (0.6-1.2 μmol) was dissolved in a mixture of 600 μl Freon-11 and 100 μl dry acetic acid. [^{18}F]F_2 was bubbled through this mixture at room temperature. Freon-11 was evaporated using neon flow at room temperature and HPLC eluent was added to the residue.

[^{18}F]CFT was purified by semi-preparative HPLC with a μBondapak C18 column. A UV absorption detector at λ=215 nm and a 2 x 2-inch NaI(Tl) crystal for radioactivity detection were used. The column was eluted with 0.01 M H_3PO_4/CH_3CN (7/3). The fraction containing the [^{18}F]CFT was collected and dried with a vacuum evaporator. For final formulation, the fraction was dissolved into 0.9% NaCl/0.1 M phosphate buffer (3/2, v/v) and passed through a sterile filter into the product vial.

4.1.5. Quality of radiopharmaceuticals

The amount of radioactivity, the pH, and the volume of the end products were measured. A sample from the product containing [^{18}F]FDOPA or [^{18}F]CFT was evaluated using analytical HPLC connected to UV and radioactivity detectors. Determinations of chemical purity, RCP, and SA were carried out by comparing HPLC

retention times and peak intensities to a reference compound of known concentration. RCYs were calculated from the initial amount of $[^{18}F]F^-$ and were decay-corrected to EOB. The SA of the product was decay-corrected to EOS.

Enantiomeric purity of the [^{18}F]FDOPA end product was determined on a CrownPak CR (+) HPLC column (150 x 4 mm, 5 µm, Daicel Chemical Industries LTD., Tokyo, Japan) eluted with 0.02 M $HClO_4$ (aq) at 0.7 ml/min. Tin contamination of the [^{18}F]FDOPA product was analyzed from selected batches by inductively-coupled plasma atomic absorption spectroscopy at the Department of Analytical Chemistry, University of Åbo Akademi, Turku, Finland. Microbiological quality of the final product was confirmed by testing sterility and bacterial endotoxins from selected experiments. These tests were performed by the Turku University Hospital Pharmacy, Turku, Finland.

As a comparision of radioHPLC and LC/MS, the SA of the [^{18}F]CFT end product was also determined with LC/MS using a PE SCIEX API 150 EX mass spectrometer (Perkin Elmer SCIEX, Toronto, Canada) equipped with a turbo ion spray source, series 200 micro pump (Perkin Elmer Instruments, CT, USA), and Symmetry C18 column (Waters Corp.). The column was eluted with MeOH/0.2% HCOOH (aq). The [^{19}F]CFT mass concentration was measured using the same reference used with the analytical HPLC. The analyses were performed in positive selected ion monitoring mode for m/z = 278 (corresponding to the protonated molecule $[MH^+]$ of [^{19}F]CFT), and the SAs were decay-corrected to EOS.

4.2. Preclinical studies with [^{18}F]FDOPA and [^{18}F]CFT

4.2.1. Experimental animals (III, IV)

Sprague-Dawley rats (Harlan Sprague-Dawley, Indianapolis, IN, USA) were housed under standard conditions (temperature 21 ºC; relative humidity 55 ± 5%, 12 hours light/dark cycle). Animal care was in accordance with the guidelines of the International Council of Laboratory Animal Science. The animals underwent momentary CO_2 sedation prior to the injection of radiotracers or pretreatments. For PET imaging, the animals were anesthetized with 2% isoflurane in oxygen. The studies were approved by the Turku University Ethics Committee for Animal Experiments and the Animal Experiment Board of the Province of Southern Finland.

The lesioning of the nigrostriatal dopaminergic pathways of the animals used in study IV was performed at Orion Pharma (Orion Corp., Turku, Finland) by injecting 6-hydroxydopamine (6-OHDA) unilaterally into the left medial forebrain bundle. Control animals were otherwise treated identically, but were injected with saline instead of 6-OHDA.

4.2.2. Biodistribution (III, IV)

Radiopharmaceuticals were injected into the tail vein of sedated rats. In study IV, the animals were premedicated with entacapone and carbidopa (both from Orion Pharma, Orion Corp.) half an hour before the [^{18}F]FDOPA injection. The animals were killed in a carbon dioxide chamber at a specified time point after injection of the radiopharmaceutical. The brains were rapidly removed and a piece of the cerebellum of each brain was dissected, measured for ^{18}F-activity in a calibrated NaI(Tl) well counter, and weighted. After decay correction, these data, expressed as the percentage of injected dose per gram of tissue (% ID/g), were used to calibrate the absolute uptake of radioactivity in autoradiographic brain images. The rest of the brain was frozen for sectioning with a cryomicrotome to 20-μm-thick coronal sections. The sections were thaw-mounted onto microscope slides, air dried, and apposed to an imaging plate for 4 hours. The imaging plates were scanned with the Fuji Analyzer BAS-5000 (Fuji Photo Film Co., Ltd., Tokyo, Japan).

Digital autoradiographic images were analyzed for count density (PSL/mm^2) with a computerized image analysis program (Tina 2.1, Raytest Isotopenmessgeräte, GmbH, Straubenhardt, Germany). Regions of interest in study III were drawn over the frontal cortex, striatum, LC, and cerebellum. Regions of interest in study IV were drawn over the left/right striatum, left/right SN, and cerebellum. The brain areas were anatomically identified from the cryomicrotome sections using a rat brain atlas (Paxinos and Watson, 1986). The count densities for background areas were subtracted from the image data. PSL/mm^2 values were converted into % ID/g values.

Other organs and tissue samples were rapidly dissected, weighted, and measured for ^{18}F-radioactivity. The decay-corrected uptake of ^{18}F-radioactivity in organs and tissues was expressed as % ID/g.

4.2.3. Pharmacological studies (III, IV)

In study III, the specificity of [^{18}F]CFT binding to DAT in the brains of pretreated rats was assessed with the selective DAT antagonist GBR12909 (Sigma-RBI, St. Louis, MO, USA). Selectivity was examined by injecting rats with fluoxetine (Sigma-RBI), a selective antagonist for SERT, or nisoxetine (RBI, Natick, MA, USA), a selective antagonist for NET. All drugs were injected intravenously into rats 60 min prior to the injection of [^{18}F]CFT. The rats were killed in a carbon dioxide chamber 40 min after the injection of [^{18}F]CFT, and the brains and organs were handled as described in section 4.2.2. The regional distribution of ^{18}F-radioactivity in the brains was determined using digital autoradiography.

In study IV, the division of the animals into groups based on circling behavior after pharmacological challenge was performed at Orion Pharma (Orion Corp.). The circling behavior of lesioned and control animals was measured after apomorphine, amphetamine, or L-DOPA injections.

4.2.4. In vivo PET imaging (III)

PET scans were carried out using an Inveon multimodality PET/computed tomography (PET/CT, Siemens Medical Solutions USA, Knoxville, TN, USA) designed for rodents and other small animals. The device provides 159 transaxial slices, a 10.0-cm transaxial field of view, and a 12.7-cm axial field of view. Following the transmission scan for attenuation correction using the CT modality, an emission scan was acquired for 120 min in 3D list mode with an energy window of 350-650 keV. The scans started immediately after intravenous injection of [^{18}F]CFT. List mode data were stored in 3D sinograms, which were then Fourier-rebinned into 2D sinograms (45 frames: 20 x 15 s, 15 x 600 s, 10 x 600 s). The image was reconstructed using 2D-filtered back-projection with a 0.5-mm ramp filter with cut-off at the Nyquist frequency. Regions of interest were placed on the striatum, cerebellar cortex, frontal cortex, and liver using Inveon Research Workplace Image Analysis software (Siemens Medical Solutions, USA) and with a CT template as an anatomical reference.

4.2.5. Dosimetry (III)

The animal % ID/g tissue data were extrapolated to humans using the % kg/g method (Kirschner et al. 1975) in which the animal % ID/g value is first multiplied by the animal's weight and then multiplied by the human organ weight/human weight ratio. The human radiation dose was estimated from these values using OLINDA/EX 1.0 software (Stabin et al. 2005).

4.2.6. Immunohistochemical staning (IV)

Dopaminergic neurons in the SN were detected by the immunohistochemical ABC technique (Hsu and Raine, 1981; Hsu et al., 1981) from the same brain cryomicrotome sections used for digital autoradiography. After digital autoradiography, the sections were fixed with acetone, endogenous peroxidase activity was blocked with hydrogen peroxide, and nonspecific background staining was reduced with normal horse serum (Vectastain ABC Kit, mouse IgG, PK-4002, Vector Laboratories, Burlingame, CA, USA). Mouse monoclonal antibody directed against TH (Boehringer Ingelheim Bioproducts Partnership, Heidelberg, Germany) was used as a primary antiserum. Brain sections were incubated with the primary antibody and then with the biotinylated secondary antibody (Vectastain ABC Kit) containing normal rat serum. Vectastain A reagent (avidin) and B reagent (biotinylated horseradish peroxidase) were mixed and allowed to stand to achieve complexation before incubation with brain sections. Diaminobenzidine, a brown endproduct at the site of the target antigen, formed upon oxidation. The number of TH-immunopositive neurons in the SN was counted using a light microscope from at least four sections per animal.

4.3. Data analysis and statistical procedures (II, III, IV)

In study II, the statistical analyses were performed with Graph Prism version 5.01 (GraphPad Software, San Diego, CA, USA). Comparison of RCYs was carried out with unpaired two-tailed Student's *t*-tests.

In study III, the statistical analyses were performed with SPSS Statistics 17.0 (SPSS Inc., Chicago, IL, USA). Comparison of SAs was carried out using paired, two-tailed Student's *t*-tests. Effects of the pretreatments were tested using repeated-measurement analysis of variance (ANOVA).

In study IV, the statistical analyses were conducted with SAS System for Windows 8.01 (SAS Institute, Cary, NC, USA). *P*-values reported from multiple comparisons were Tukey-Kramer adjusted. Striatum and SN were analyzed with ANOVA for the design of four parallel groups with replicated measurements from each side. The statistical model consisted of the fixed effects for treatment group, side, replicate, and all of their interactions. In the case of a significant treatment-group, treatment-by-side, or treatment-by-replicate interaction effect, the analysis was continued with pairwise comparisons using linear contrasts within the same model. Cerebellum was analyzed with a similar model, excluding the side effect. The normality of the distributions was tested with the Shapiro-Wilk test for normality.

Measurements in all studies are expressed as means ± standard deviation (SD) for the indicated number of observations. Means were considered significantly different when $p < 0.05$.

5. RESULTS

5.1. Production of radiopharmaceuticals

5.1.1. Synthesis of [^{18}F]FDOPA (I,II,IV)

[^{18}F]FDOPA (**7**) was prepared according to the synthetic scheme presented in Fig. 5.1. Freon-11 was used as a solvent in studies I and IV; in study II, CCl_3F, $CDCl_3$, CD_2Cl_2, C_3D_6O, $CHCl_3$ stabilized with amylene, CH_2Cl_2 stabilized with amylene, and C_3H_6O were used as solvent. The results for RCY and SA from studies I and II are summarized in Table 5.1. The initial [^{18}F]F$^-$ activity was 33 ± 4 GBq and 20 ± 6 GBq in studies I and II, respectively. The average synthesis time was 50 ± 3 min, including the synthesis of [^{18}F]F_2, radiofluorination, evaporation of the solvent, removal of the protecting groups, semi-preparative purification, and formulation of the final product. In a typical semi-preparative HPLC purification, the [^{18}F]FDOPA collected from the fraction eluting at the retention time of 10.5 min was sterile filtered, at which point it was ready for human use. The radioactivity of [^{18}F]FDOPA produced for clinical imaging in study I varied from 1008 MBq to 2580 MBq (1544 ± 400 MBq) at EOS.

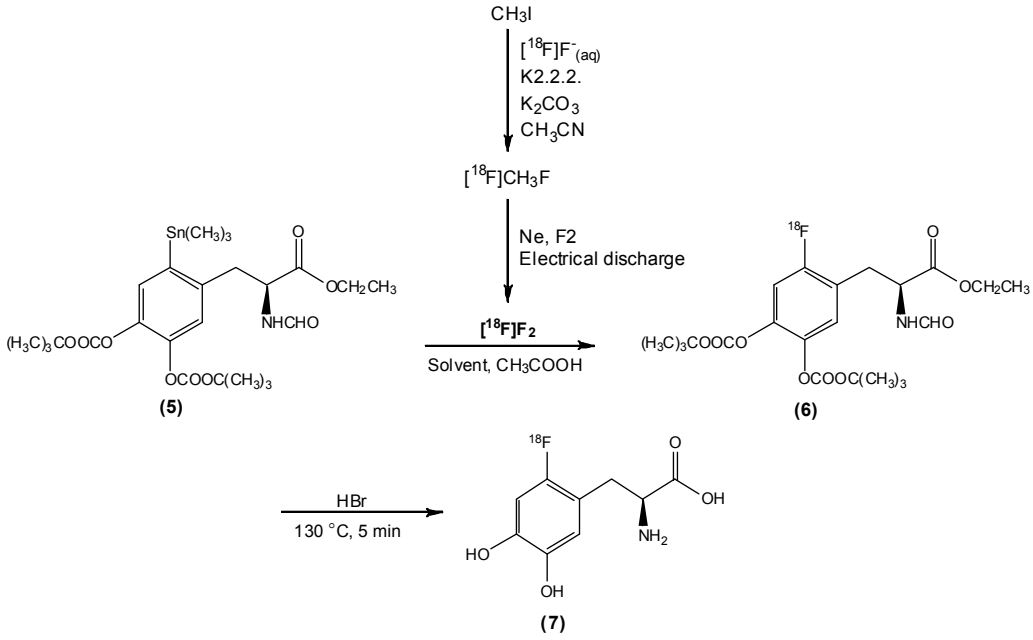

Figure 5.1. Scheme of the synthesis of [^{18}F]FDOPA **(7)**. Solvent was either Freon-11, CCl_3F, $CDCl_3$, CD_2Cl_2, C_3D_6O, $CHCl_3$ stabilized with amylene, CH_2Cl_2 stabilized with amylene, or C_3H_6O.

Analytical HPLC indicated that the RCP exceeded 98% and the chemical purity with respect to 6-L-DOPA was greater than 95% in all cases. The final product was sterile and endotoxin-free, and it was radiochemically stable for up to six hours. The enantiomeric purity exceeded 99%. The tin concentration of the final product varied from 5.8 µg/l to 12.6 µg/l (n=5), with the bulk of the tin eluting in the void fraction.

Table 5.1. The RCY and SA of [^{18}F]FDOPA using various solvents in electrophilic fluorination.

Solvent	n	RCY[1] [%]	SA[2] [GBq/µmol]
Freon-11[3]	50	6.4 ± 1.7	3.7 ± 0.9
Freon-11[4]	7	6.0 ± 1.5	2.4 ± 1.0
CD_2Cl_2	6	7.8 ± 0.6	2.7 ± 0.4
$CDCl_3$	3	7.5 ± 0.7	2.6 ± 1.1
C_3D_6O	2	8.5 ± 0.9	3.1 ± 0.03
CH_2Cl_2	1	0.9	3.4
$CHCl_3$	1	0.5	2.8
C_3H_6O	1	5.2	2.8

[1] Radiochemical yields (RCY) are calculated from the initial amount of [^{18}F]F^- and decay corrected to EOB.
[2] Specific radioactivities (SA) are corrected to EOS.
[3] Study I: initial [^{18}F]F- activity 33 ± 4 GBq
[4] Study II: initial [^{18}F]F- activity 20 ± 6 GBq

In study II, reactions in $CDCl_3$, CD_2Cl_2, or C_3D_6O with acetic acid provided better RCYs of [^{18}F]FDOPA than reactions in Freon-11. The RCYs obtained with deuterated CD_2Cl_2 and $CDCl_3$ with acetic acid were 8- and 15-fold higher, respectively, than the RCYs obtained with the corresponding non-deuterated solvents (Table 5.1). The RCY obtained with C_3H_6O was comparable to that obtained with its deuterated analog, C_3D_6O. The SA of the product exhibited little variation between different solvents. Not having acetic acid in the reaction mixture during the fluorination significantly decreased the RCY of [^{18}F]FDOPA. Two experiments with $CDCl_3$ resulted in loss of radioactivity (RCY 4.2 ± 0.9%) when compared with experiments without radioactivity loss (7.5 ± 0.7%). However, increasing the $CDCl_3$ evaporation temperature from 60 °C to 130 °C did not further affect RCY (4.0%).

5.1.2. Synthesis of [^{18}F]CFT (III, IV)

Electrophilic fluorination was applied to a stannylated precursor (**8**, Fig. 5.2) to synthesize [^{18}F]CFT (**9**, n = 24). The initial [^{18}F]F^- activity was 37 ± 3 GBq and the

average synthesis time was 43 ± 3 min, including the synthesis of $[^{18}F]F_2$, radiofluorination, evaporation of the solvent, and semi-preparative purification. In a semi-preparative HPLC purification, the [^{18}F]CFT fraction eluting at the retention time of 10.5 min was collected. Evaporation to dryness and formulation for injection took an additional 10 min.

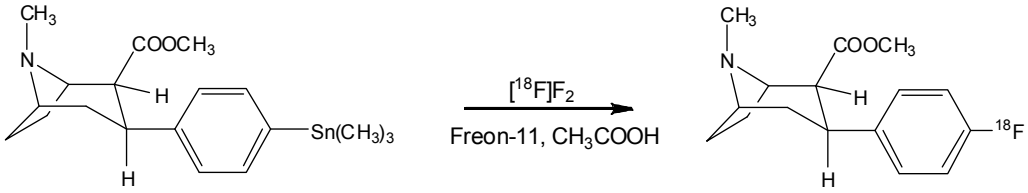

Figure 5.2. Scheme of the synthesis of [^{18}F]CFT **(9)**.

The RCY calculated from the initial amount of $[^{18}F]F^-$ (decay-corrected to EOB) was 3.2 ± 1.0% and the radioactivity of [^{18}F]CFT was 917 ± 278 MBq at EOS. The SA measured by analytical HPLC was 14.5 ± 3.4 GBq/µmol (8.9-23.6 GBq/µmol, all values decay-corrected to EOS). The RCP exceeded 99% in all HPLC studies. Chemical purity was acceptable; CFT was the only signal, in addition to the void signal, in the UV trace of the final product. The final product was radiochemically stable for up to six hours.

For selected batches (n = 19), the SA of the final product was also determined by LC/MS. The SA of these batches measured by analytical HPLC was 14.9 ± 3.1 GBq/µmol, and the SA measured by LC/MS was 16.4 ± 4.6 GBq/µmol. SAs calculated using the analytical HPLC method differed significantly from SAs calculated using LC/MS method ($p < 0.003$).

5.2. Preclinical studies with [^{18}F]FDOPA and [^{18}F]CFT

5.2.1. Biodistribution and pharmacokinetics (III)

The data on ^{18}F-radioactivity uptake in the striatum, LC, frontal cortex, and cerebellum of healthy control rats and monoamine inhibitor-pretreated rats 40 min after [^{18}F]CFT injection appear in Table 5.2. Pretreatment with GBR12909 significantly reduced the [^{18}F]CFT uptake in the striatum and LC. In nisoxetine-pretreated rats, the [^{18}F]CFT uptake decreased significantly in the LC. Fluoxetine pretreatment had no effect on the accumulation of the ^{18}F-radioactivity in any region studied.

Table 5.2. Uptake (% ID/g) of ^{18}F-radioactivity 40 min after the injection of [^{18}F]CFT into the brains of control and pretreated rats. All values are means ± SD. The effect of pretreatment was compared with the uptake values of control rats. Means were considered significantly different when $p < 0.05$.

Uptake [%ID/g]	Control n=6	GBR 12909 n=7	Nisoxetine n=6	Fluoxetine n=6
Striatum	1.55 ± 0.78	0.49 ± 0.18*	1.48 ± 0.22	1.38 ± 0.75
Locus coeruleus	0.67 ± 0.29	0.37 ± 0.11**	0.23 ± 0.05*	0.47 ± 0.16
Frontal cortex	0.32 ± 0.08	0.23 ± 0.04	0.26 ± 0.03	0.33 ± 0.13
Cerebellum	0.20 ± 0.04	0.15 ± 0.04	0.17 ± 0.02	0.23 ± 0.09

*$p < 0.01$ compared to control
**$p < 0.05$ compared to control

The striatum-to-cerebellum uptake ratio increased from 2.1 ± 0.2 at 10 min to 8.8 ± 2.2 at 120 min. The LC-to-cerebellum uptake ratio was 2.2 ± 0.3 at 10 min and 3.5 ± 1.6 at 120 min. The frontal cortex-to-cerebellum uptake ratio was constant, ranging from 1.4 to 1.6 at all time points and with all pretreatments. All monoamine inhibitors used in this study significantly decreased the LC-to-cerebellum uptake ratio 40 min after [^{18}F]CFT injection. Pretreatment with GBR12909 significantly reduced also the striatum-to-cerebellum uptake ratio (Fig. 5.3).

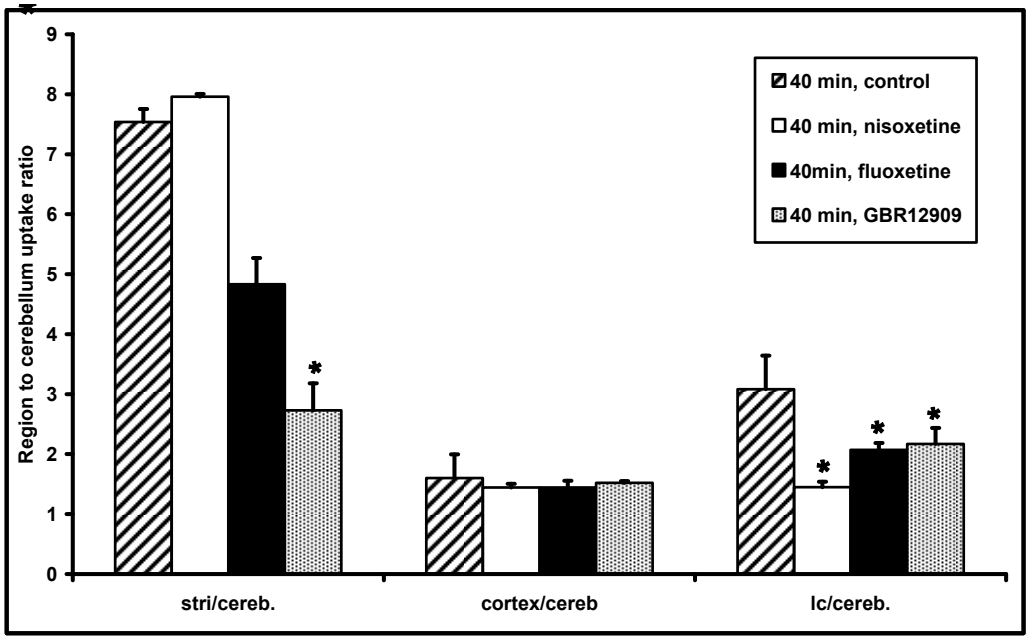

Figure 5.3. Region-to-cerebellum uptake ratios 40 min after [^{18}F]CFT injection in rats with or without pretreatment from the *ex vivo* studies. stri = striatum, lc = locus coeruleus, cereb = cerebellum. * $p < 0.05$, compared to control.

In peripheral organs and tissues, the uptake of [^{18}F]CFT-derived radioactivity peaked at 20 min after the injection of [^{18}F]CFT in most tissues and decreased thereafter. High levels of radioactivity were found in the liver, kidneys, and spleen. In the liver, the highest uptake (8.3 ± 1.2% ID/g) was recorded 120 min after injection of [^{18}F]CFT. ^{18}F-radioactivity accumulation in bone increased slowly with time, but was still low (0.19 ± 0.15% ID/g) at 120 min.

Pretreatment of the rats with GBR12909 significantly decreased the uptake of ^{18}F-radioactivity in the pancreas (without pretreatment, 0.35 ± 0.11% ID/g; with pretreatment, 0.17 ± 0.05% ID/g). No significant changes in ^{18}F-radioactivity uptake were recorded in the periphery of the rats pretreated with nisoxetine or fluoxetine.

5.2.2. In vivo PET Imaging (III)

Uptake of radioactivity in the striatum and in the cerebellum peaked during the first 5-10 min and decreased thereafter (Fig. 5.4).

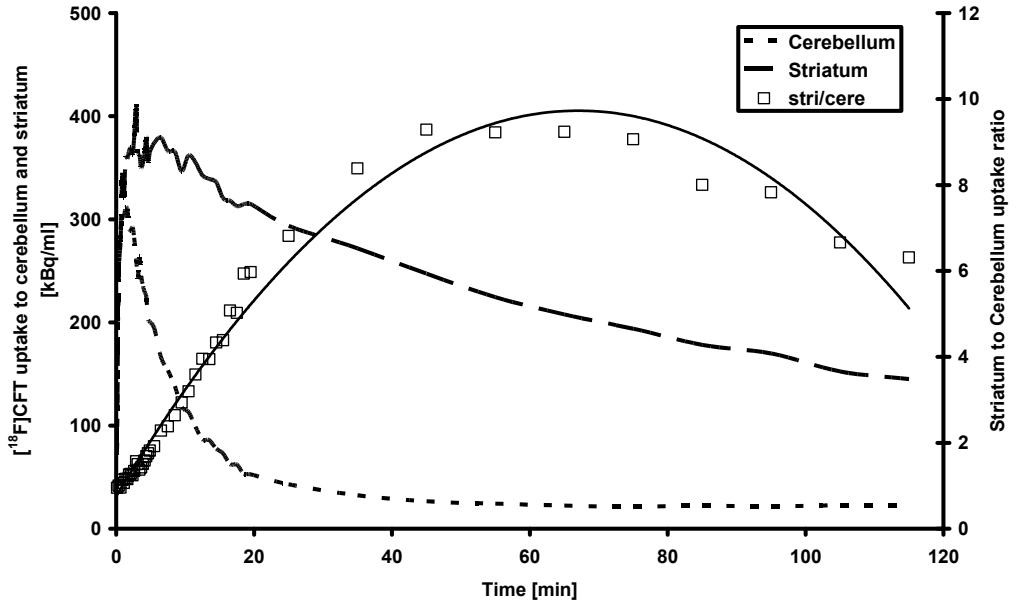

Figure 5.4. Time courses of striatum (stri) uptake, cerebellum (cere) uptake, and striatum-to-cerebellum uptake ratio from the *in vivo* animal PET study.

The striatum-to-cerebellum ratio peaked at ~9 after 60 min. The highest *in vivo* uptake of radioactivity in the periphery was observed in the kidneys in the first minutes after injection and in the liver (Fig. 5.5). The uptake increased in liver during the first 60 min of PET imaging, and was almost constant until the end of the scanning at 120 min after injection.

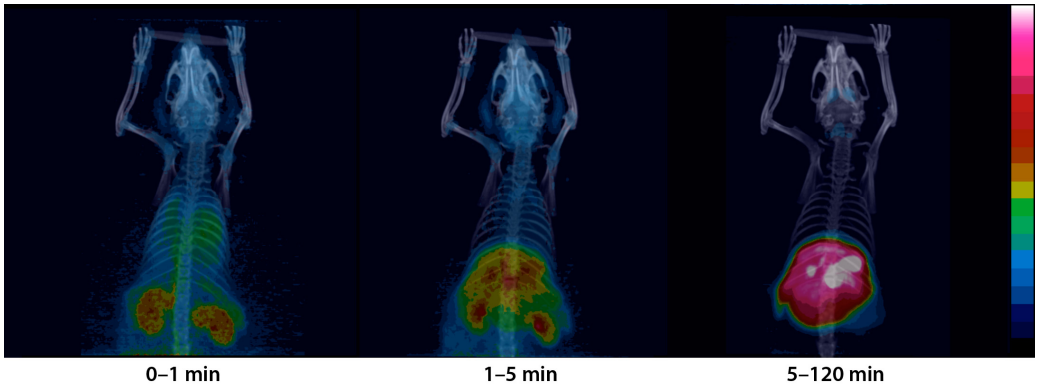

Figure 5.5. Animal PET-CT of [^{18}F]CFT accumulation in rat. Data was collected from 0-120 min post-injection. Dark blue low radioactivity, white high radioactivity.

5.2.3. Dosimetry (III)

The ED following a single injection of [^{18}F]CFT estimated for the standard human model was 9.17 μSv/MBq.

5.2.4. Behavioral tests and immunohistochemistry (IV)

In study IV, the animals were divided into groups according to circling behavior after saline, apomorphine, amphetamine, or L-DOPA challenges (control, Groups 1-3). The control animals did not exhibit preferential circling behavior for any of the assessed drugs. Group 1 displayed a clear amphetamine response, but no other responses were apparent. Group 2 showed amphetamine and apomorphine responses, but no L-DOPA response. Group 3 responded to amphetamine, apomorphine, and L-DOPA. The number of TH-immunopositive neurons (dopamine cell bodies) present in the SN was calculated from the immunohistochemically stained cryosections. The left (lesioned)-right (intact) ratio of the calculated dopaminergic cell bodies in the control animals was approximately one. Regarding the number of TH-positive cell bodies in the left and right SN, Group 1 displayed a 50% difference and Groups 2 and 3 exhibited a 90% difference (Table 5.3).

5.2.5. [^{18}F]FDOPA and [^{18}F]CFT uptake in lesioned animals (IV)

For all animals, the uptake of ^{18}F-radioactivity (% ID/g) was measured in the cerebellum in order to determine nonspecific uptake. There was no significant difference in nonspecific uptake of a tracer between the control and lesioned animals, and thus the cerebellum uptake values were grouped together in subsequent data analysis. Uptakes in the left and right striatum and the left and right SN were measured. The uptake ratios and the left-right side ratio of dopamine cell bodies in SN after immunohistochemical staining are presented in Table 5.3.

In the control animals there was no significant difference between the ^{18}F-radioactivity uptake of the left and right striata or SN. With both radioligands the left-right side ^{18}F-radioactivity uptake was significantly lower in all pharmacologically characterized groups compared to the control group. With [^{18}F]CFT, Group 1 had a significantly higher ratio in the SN but not in the striatum when compared to Groups 2 and 3. With [^{18}F]FDOPA, there were no significant differences in ratios in any of the groups. Neither [^{18}F]CFT nor [^{18}F]FDOPA injection led to any significant differences between Groups 2 and 3.

Table 5.3. Radioactivity uptake ratios of the lesioned side and intact side after the injection of [^{18}F]CFT or [^{18}F]FDOPA in the striatum and in the SN, as well as the lesioned-intact side ratio of dopaminergic cell bodies (DA cell ratio) in the SN after immunohistochemical staining (all values mean ± SD). Percent decreases of the mean uptake in the lesioned side versus the intact side (L/R) and the decrease of the uptake in the lesioned side as compared to the mean uptake of the control group (L/S) are also presented.

	[^{18}F]CFT uptake ratios		[^{18}F]FDOPA uptake ratios		DA cell ratio
	Striatum	**SN**	**Striatum**	**SN**	**SN**
Control	0.81 ± 0.13	0.92 ± 0.06	1.10 ± 0.16	1.04 ± 0.03	0.91 ± 0.15
Group1	0.38 ± 0.30	0.62 ± 0.09	0.86 ± 0.11	0.87 ± 0.01	0.50 ± 0.28
Group2	0.13 ± 0.04	0.46 ± 0.06	0.75 ± 0.07	0.86 ± 0.03	0.08 ± 0.06
Group3	0.13 ± 0.03	0.48 ± 0.02	0.74 ± 0.02	0.80 ± 0.03	0.06 ± 0.03
L/R	81 %	49 %	23 %	16 %	n.a.
L/S	71 %	48 %	31 %	25 %	n.a.

n.a. not analyzed

The left-right ratio of the number of dopaminergic neurons present in the SN plotted against the left-right ratio of [^{18}F]CFT or [^{18}F]FDOPA uptake in both striatum and SN showed good correlation (see paper IV, Fig. 3). In the striatum, both radioligands exhibited a linear correlation between individual apomorphine response and the left-right radioactivity uptake ratio. There was no significant correlation regarding the L-DOPA response to the radioactivity uptake. The amphetamine response correlated better with the left-right uptake ratio in [^{18}F]CFT studies than in [^{18}F]FDOPA studies.

6. DISCUSSION

6.1. Synthesis of [^{18}F]FDOPA

New diagnostic uses of [^{18}F]FDOPA for the imaging of neuroendocrine tumors and hyperinsulinemia in infants have brought interest in simple and reproducible methods to produce the compound in large quantities. The drawbacks in the established methods of [^{18}F]FDOPA production included the complexity of the nucleophilic method and the poor SA achieved with the electrophilic method. As a consequence of this low SA, the chemical manipulations are difficult and involve large amounts of expensive precursor, large amounts of the restricted solvent Freon-11, and difficult separation processes due to the large amounts of starting material. Inefficient production of electrophilic labeling agents has restricted the use of the electrophilic method. Fluorodestannylation by post-target-produced [^{18}F]F_2 with moderately high SA offers a solution to these problems. The post-target production of [^{18}F]F_2 has been developed at the Turku PET Centre (Bergman and Solin 1997), a method unique for Turku.

In the investigations presented in this thesis, [^{18}F]F^- was produced by the common ^{18}O(p,n)^{18}F reaction using $H_2{}^{18}O$ as a target; [^{18}F]F_2 was generated post-target using a fully automated synthesis device. The [^{18}F]F_2 was bubbled through 4 μmol of stannylated precursor dissolved in 700 μl Freon-11 at room temperature. Acetic acid was added to the reaction solution just before [^{18}F]F_2 bubbling to make [^{18}F]F_2 more susceptible to the substitution reaction. In study II, the RCY was significantly increased by adding 25 μl acetic acid in the reaction mixture, but no additional benefit was achieved with a larger volume (50 μl) of acetic acid because both amounts were in great molar excess to the reactants. Protecting groups were hydrolyzed with HBr as in previous studies, but less HBr was used and the hydrolysis time was reduced to 5 min; in a previous work (de Vries et al. 1999) involving higher molar amounts of all reactants, a hydrolysis time of less than 10 min resulted in incomplete hydrolysis. After neutralization, the volume of the reaction mixture was adequate for semi-preparative purification. NaCl solution (0.9%) containing 0.01% acetic acid was used as an eluent and only sterile filtration was required before human injection. The tin concentration of the final product was low; the highest measured tin concentration of the final product was 12.6 μg/l, with a maximal permitted amount of 500 μg/V (V being the maximum recommended dose in milliliters) according the European Pharmacopoeia or 500 μg/l according to The United States Pharmacopeia.

In addition to easier semi-preparative purification, smaller amounts of reagents offer other advantages. For example, the evaporation of Freon-11 before hydrolysis is fast and does not require vacuum or elevated temperature. The minimization of Freon-11 use is important due to the harmful effects of Freon-11 in the atmosphere. In study II, CD_2Cl_2, $CDCl_3$, and C_3D_6O were all found to be suitable solvents for replacing Freon-11 in the electrophilic synthesis of [^{18}F]FDOPA. All deuterated solvents generated

better RCYs of [^{18}F]FDOPA than Freon-11. Gas-liquid reaction dynamics are a complex sum of many factors affecting the kinetics of reactions (Akita and Yoshida 1974, Schroeder and Troe 1987). Thus it is difficult to find any simple explanation for the better RCYs in the synthesis of [^{18}F]FDOPA using other solvents than Freon-11. However, in this context the chemical purity of the solvents is of paramount importance. Heating of the reaction vessel was required to evaporate solvents with boiling points higher than Freon-11 in a reasonable time; if the evaporation temperature was too high (near or above the boiling point of the solvent), the amount of radioactivity in the reaction vessel decreased radically during evaporation in the present experiments. Investigations performed in $CDCl_3$ were the most sensitive to loss of radioactivity due to elevated evaporation temperature, likely from the relatively high boiling point. With $CHCl_3$ and CH_2Cl_2, [^{18}F]F_2 reacted with the double bond in the amylene stabilizer and unidentified volatile radioactive by-products were formed, decreasing the overall RCY. Due to the high reactivity of [^{18}F]F_2, additives such as stabilizers and impurities in commercially available reagents and solvents will decrease the RCY of the final product during electrophilic fluorination. Commercially available acetone does not contain stabilizers that can react with [^{18}F]F_2, and thus the RCY using C_3H_6O was higher than that resulting from use of $CHCl_3$ or CH_2Cl_2.

The present results were in good agreement with earlier studies using $CHCl_3$ or $CDCl_3$ as a solvent in electrophilic fluorination (Füchtner et al. 2008). Paper II demonstrated that CD_2Cl_2 and C_3D_6O were also suitable solvents for electrophilic fluorination. Currently, CD_2Cl_2 is used in the routine production of [^{18}F]FDOPA in the Turku PET Centre due to the good reproducibility of the method presented in study II.

In the method used in studies I, II, and IV, [^{18}F]F_2 was post-target-produced from [^{18}F]F^- and the RCYs were calculated from the initial amount of [^{18}F]F^-. The RCYs in the other electrophilic production routes (section 2.4.3) are calculated from in-target-produced [^{18}F]F_2. Due to this difference in calculation, the RCYs presented in this study are lower than in the other electrophilic production routes (section 2.4.3).

The SA of [^{18}F]FDOPA achieved with post-target-produced [^{18}F]F_2 was considerably higher (~3300-fold increase) than that achieved using [^{18}F]F_2 produced by the ^{20}Ne(d,α)^{18}F reaction (Tables 2.3. and 5.1.). The SA of [^{18}F]F_2 generated by the ^{18}O(p,n)^{18}F reaction using $^{18}O_2$ target is higher than the [^{18}F]F_2 produced by the ^{20}Ne(d,α)^{18}F reaction, but is ten-fold lower than that produced by the method presented in this study. There are no published data regarding the production of [^{18}F]FDOPA with $^{18}O_2$ as a target. In study II the SA of the product exhibited little variation between different solvents, demonstrating the reproducibility of the conversion of [^{18}F]F^- to [^{18}F]F_2. Even though the high SA of [^{18}F]FDOPA is not crucial for human studies, it enhances the quality of PET data and decreases the pharmacological dose for patients. SA can be increased by decreasing the amount of carrier fluorine (F_2) used in the ^{18}F/^{19}F exchange reaction, but then the RCY decreases. SA can also be increased by increasing the initial [^{18}F]F^- activity. The CC-18/9 cyclotron (Efremov Institute of

Electrophysical Apparatuses) installed in the Turku PET Centre produces greater initial [^{18}F]F$^-$ activity than was possible with the old MGC-20 cyclotron. In recent clinical productions in the Turku PET Centre starting from [^{18}F]F$^-$ produced in the CC-18/9 cyclotron, the SA of [^{18}F]FDOPA varies from 7 to 8 GBq/μmol.

The synthetic route presented in study II is reproducible and [^{18}F]FDOPA is produced on average once per week in the Turku PET Centre for clinical use. Two to five human studies with injected doses up to 250 MBq may be performed from a single synthesis. The quality of the final product, which is analyzed from every synthesis before human injection, is reproducible from synthesis to synthesis.

6.2. Synthesis of [^{18}F]CFT

To the best of my knowledge, [^{18}F]CFT is at present the only neurotransporter or neuroreceptor tracer available that is synthesized via electrophilic fluorination. Post-target-produced [^{18}F]F_2 offers a feasible method for generating PET tracers with high SA for neuroimaging through electrophilic fluorination. The SA of [^{18}F]CFT can potentially be increased by further optimization of this ^{19}F-^{18}F exchange reaction by decreasing the amount of carrier F_2. However, this change resulted in a dramatic decrease in RCY. The amount of carrier F_2 used in studies III and IV (290-400 nmol) is a compromise, offering SA and RCY high enough for several human PET studies from one production run. The radiochemical and chemical purity of the final product were verified by HPLC and fulfilled the requirements for intravenous use in humans that is RCP exceeded 99 % in all syntheses (the acceptance limit was 95 %) and there was no unknown signals in the UV trace of the final product.

For radioligands with very high SA, the sensitivity limitation of UV detection means that LC/MS is the only method for measuring SA. In study III, in which [^{18}F]CFT was synthesized through electrophilic fluorination at high specific activity, the determination of SA was compared for HPLC/UV absorption and LC/MS. Quantitative analyses indicate that LC/MS is a faster and more sensitive method than HPLC equipped a UV detector. However, LC/MS is more easily affected by changes in the sample matrix. In study III, the SAs were higher when determined by LC/MS than by HPLC. The CFT concentration was lower when measured by LC/MS than by HPLC, which may be due to ion suppression in the LC/MS (Annesley 2003). The effect of ion suppression may be diminished by more extensive chromatographic separation or by sample preparation prior to mass spectrometry. However, both methods are suitable for analysis in the present case.

6.3. [^{18}F]CFT: pharmacokinetics and dosimetry

In the biodistribution study of [^{18}F]CFT in rats, the highest level of radioactivity was identified in the main excretory organs. The uptake in bone was low even at 120 min,

reflecting good stability of the carbon-fluorine bond. Radioactivity accumulated in the liver with the maximum value at 120 min, indicating slow excretion and low metabolism. The biodistribution results from the *in vivo* study were in accordance with *ex vivo* findings.

In the periphery, non-neuronal DAT expression and DAT immunoreactivity have been found in the stomach, pancreas, and kidneys (Eisenhofer 2001). [^{18}F]CFT uptake in the pancreas, stomach, and kidneys was moderate in study III. No NET- or SERT-specific binding of ^{18}F-radioactivity occurred in the periphery, even though extraneuronal NET expression was previously reported in the lung, adrenal medulla, and placenta (Eisenhofer 2001). After GBR12909 pretreatment, the radioactivity uptake decreased significantly in the pancreas, indicating DAT-specific binding.

In the brain, radioactivity uptake in the striatum was specific for DAT since it significantly decreased with GBR12909 pretreatment. In addition to DAT, the striatum contains a low density of SERT, and NET is virtually absent (Hoffman et al. 1998). Neither fluoxetine nor nisoxetine pretreatment affected radioactivity uptake in the striatum. High radioactivity accumulation was observed in the LC, a brain region with high NET density, but this accumulation was significantly decreased in rats pretreated with nisoxetine, indicating that NET sites bind [^{18}F]CFT. The affinity of CFT for DAT and NET is of the same order of magnitude. However, since NET is virtually absent in the striatum, [^{18}F]CFT is suitable for imaging striatal DAT sites. The accumulation of radioactivity in the LC also significantly decreased in rats pretreated with GBR12909. The relatively high dose of GBR12909 used in the pretreatment of the animals suggests that although the affinity of GBR12909 for NET is 50-fold less than for DAT, this dosage is high enough to displace [^{18}F]CFT from the NET sites in the LC. It is noteworthy that the *p*-value in the statistical analyses was higher for the LC than for the striatum in the GBR12909 blocking study.

In the *ex vivo* study, the uptake ratios for the striatum, LC, and cortex versus the cerebellum reached a maximum between 40 and 120 minutes. In the *in vivo* study, the maximum striatum-to-cerebellum ratio appeared after 60 min. The absolute values of this ratio were similar in these two studies, ranging from 9-10. It is worth mentioning that the small LC cannot be analyzed from the *in vivo* PET study due to the limited resolution and the partial volume effect of the PET imaging devices. On the other hand, the entire time course of tracer uptake can be obtained from a single study using the *in vivo* method. These parallel studies provide a good demonstration of the strengths and weaknesses of different methods in radiopharmacological studies. Overall, the distribution of radioactivity in rats after [^{18}F]CFT injection was in good agreement with our earlier preliminary studies (Haaparanta et al. 1996, Marjamäki et al. 2009) and with studies using [^{3}H]CFT (Kaufman and Madras 1993, Scheffel et al. 1991).

The human ED value for [^{18}F]CFT (9.17 μSv/MBq) is consistent with values measured with another dopamine transporter ligand, ^{18}F-FPCIT (Robeson et al. 2003).

Extrapolation of the animal data to estimate the human radiation dose is inexact, but the order of magnitude of the ED value for [^{18}F]CFT correspond well with those of other ^{18}F-labeled radioligands.

6.4. Dopamine dysfunction in the rat brain measured with [^{18}F]FDOPA and [^{18}F]CFT

In study IV, the number of surviving nigral dopaminergic neurons in a 6-OHDA rat model of unilateral PD was evaluated with [^{18}F]FDOPA and [^{18}F]CFT. Striatal uptake of [^{18}F]FDOPA and [^{18}F]CFT was sufficiently sensitive for detecting dopaminergic hypofunction. Since the uptake of [^{18}F]FDOPA and [^{18}F]CFT reflect different aspects of dopaminergic function, their ability to reflect the number of functional nigral neurons may differ. The radioligand experiments were conducted *ex vivo* with pharmacologically characterized animal groups; the severity of the nigral lesion was categorized according to the behavioral response of the rats to direct or indirect dopaminergic agonists. By including rats with different behavioral responses to dopaminergic drugs, rats with varying degrees of nigrostriatal lesion were obtained, making correlation analyses feasible. The severity of nigral lesion was confirmed by counting the TH-immunopositive neurons in the SN.

Study IV indicated that [^{18}F]CFT is more sensitive than [^{18}F]FDOPA for detection of the degree of nigral lesion. In all lesioned groups, the decline of striatal uptake of [^{18}F]CFT was significantly greater than the decline of [^{18}F]FDOPA uptake. Compensatory changes of dopaminergic system may occur, as described in PD patients in whom the ratio of homovanillic acid (the main metabolite of DA) to DA in the cerebrospinal fluid increased (Bernheimer et al. 1973), indicating that the remaining dopaminergic neurons try to compensate for neuronal loss by increasing their turnover rate. These compensatory changes have more effect to [^{18}F]FDOPA uptake than to [^{18}F]CFT uptake. Also, the significant correlation between [^{18}F]CFT uptake and response to amphetamine that causes circling in rats with relatively mild nigral lesions indirectly suggests that [^{18}F]CFT is more sensitive than [^{18}F]FDOPA for revealing mild nigral lesions, at least in this animal model. When ligand uptake was compared with behavioral response, it was noted that the greater the reduction in [^{18}F]FDOPA or [^{18}F]CFT uptake, the stronger the response to apomorphine. This observation is in accordance with behavioral data showing that apomorphine response occurs with extensive nigral lesions (Sarre et al. 1992). However, the behavioral response to L-DOPA did not seem to be associated with the degree of reduction of either [^{18}F]FDOPA or [^{18}F]CFT uptake in the striatum, indicating that there are factors other than the nigrostriatal lesion that affect L-DOPA response. For instance, compensatory changes in receptors and alteration in the function of presynaptic dopaminergic terminals may be involved.

The main pathophysiological process in PD is a progressive loss of nigral dopaminergic neurons. Thus, by investigating striatal uptake of [^{18}F]FDOPA or [^{18}F]CFT, the degree of nigral damage can be indirectly estimated, especially its change over time. Study IV demonstrated that [^{18}F]FDOPA and [^{18}F]CFT uptakes in the striatum in a rat model of PD reflect the actual number of neurons in the SN, but [^{18}F]CFT seemed to be more sensitive in this respect. Although progressive nigral destruction in human PD differs from the rather acute lesion in the 6-OHDA rat model, the present findings suggest that these tracers are useful for disease detection and follow-up and to monitor the effect of various interventions on disease progression.

6.5. Future aspects

Several laboratories are at present establishing their own modifications of the post-target-production of [^{18}F]F_2. This progress, as well as the development of novel ^{18}F-labeled stable and selective electrophilic fluorination agents such as [^{18}F]selectfluor (Teare et al. 2010), can make electrophilic fluorination a practical and widely used method for the generation of numerous ^{18}F-labeled radiopharmaceuticals with high SA. Furthermore, development of a method to produce a NCA electrophilic ^{18}F-labeling agent is of high interest. [^{18}F]FCl, an ^{18}F-labeling agent appropriate for aliphatic addition of ^{18}F to a double bond, can in theory be produced without carrier. Carrier-added [^{18}F]FCl has already been employed successfully in the incorporation of ^{18}F to a double bond to produce a chlorinated analogue of EF5 (Kirjavainen et al. unpublish data). The development of a NCA method to produce [^{18}F]FCl is currently in progress at the Turku PET Centre.

The observation that [^{18}F]CFT exhibits specific uptake in the pancreas warrants future studies in humans with respect to potential utility in pancreatic imaging. In addition, the ability of nisoxetine to block [^{18}F]CFT binding in the LC suggests that [^{18}F]CFT may also be used as a NET ligand.

7. CONCLUSIONS

The major conclusions of the work presented in this thesis are:

1. Post-target-produced [^{18}F]F_2 was successfully used as a labeling agent in fluorodestannylation to produce [^{18}F]FDOPA. The reagent amounts used in this synthesis are considerably reduced versus other electrophilic labeling approaches, simplifying the necessary manipulations during synthesis and purification.

2. Deuterated dichloromethane, deuterated chloroform, and deuterated acetone were all found to be suitable solvents for the electrophilic synthesis of [^{18}F]FDOPA. These compounds provided better yields than Freon-11, and the end products fulfilled quality requirements for patient injection.

3. Adding acetic acid to the reaction mixture prior to electrophilic labeling in the synthesis of [^{18}F]FDOPA significantly increased the RCY, but no additional benefit was achieved when a larger volume of acetic acid was used.

4. Post-target-produced high SA [^{18}F]F_2 was used to incorporate ^{18}F directly into the phenyl ring of [^{18}F]CFT. The end product exhibited high radiochemical and chemical purity and a sufficiently high SA for use in *in vivo* neurotransmitter studies.

5. [^{18}F]CFT uptake in the striatum was specific for DAT. In the LC, [^{18}F]CFT displayed specific binding to NET and therefore is suitable for imaging NET. In the periphery, DAT-specific binding occurred in the pancreas.

6. The ED value for [^{18}F]CFT corresponded well with those of other ^{18}F-labeled radioligands.

7. Both [^{18}F]FDOPA and [^{18}F]CFT clearly demonstrated nigrostriatal dopaminergic hypofunction and correlated with the number of nigral dopaminergic neurons in 6-OHDA lesioned rats. [^{18}F]FDOPA showed a much higher non-specific uptake of radioactivity due to extensive metabolism. Therefore, [^{18}F]FDOPA was less sensitive than the DAT tracer [^{18}F]CFT in detecting these defects.

8. ACKNOWLEDGEMENTS

This work was carried out at the Radiopharmaceutical Chemistry Laboratory and at the MediCity Research Laboratory of the Turku PET Centre, University of Turku.

I thank Professor Juhani Knuuti, the director of Turku PET Centre and Professor Jaakko Hartiala at the Department of Clinical Physiology and Nuclear Medicine for the facilities and for the opportunity to complete this work.

I owe my greatest gratitude to my supervisors Professor Olof Solin and Docent Merja Haaparanta-Solin for introducing me to everything from the production of radionuclides to preclinical studies. You have been amazingly encouraging and patient during all these years.

I warmly thank Eeva-Liisa Kämäräinen, PhD and Jacek Koziorowski, PhD for their constructive comments and criticism after reviewing this thesis.

I thank all my co-authors. Especially, I would like to thank Professor Juha Rinne for his great expertise in the field of neurology and Antti Haapalinna, PhD and Riitta Niemi, MSc from Orion Pharma for their contribution to study VI.

I am sincerely thankful to the personnel at the Accelerator Laboratory of Åbo Akademi University for excellent radionuclide production: Docent Sven-Johan Heselius, Stefan Johansson, Per-Olof Eriksson, Erkki Stenvall, Johan Rajander, and Jussi Aromaa. I also thank Esa Kokkomäki, Simo Vauhkala, and Timo Saarinen for technical support and the Laboratory Service unit: Nina Lauren, Margit Åhman-Kantola, and Marja-Liisa Pakkanen for taking care of the whole laboratory. Marko Tättäläinen and Rami Mikkola are acknowledged for their help in all my computer problems.

I am very grateful to Tove Grönroos, Päivi Marjamäki, and Tarja Marttila for their professional guidance and help in the preclinical studies during very long and busy days (without any coffee breaks).

I express special thanks to Jörgen Bergman for his pioneering work for our laboratory and his invaluable scientific advice. I also warmly thank Olli Eskola for looking after me at the beginning and for the amusing atmosphere in the laboratory. Pertti Lehikoinen, Tapio Viljanen, and Semi Helin are acknowledged for sharing their knowledge in radiochemistry, and Pirjo Rautiainen and Riikka Kivelä for their supervision in quality issues.

Eveliina Arponen, Anna Kirjavainen, Paula Lehtimäki, Riikka Purtanen, Johanna Rokka, Enni Saksa, Piritta Saipa, Nina Savisto, and Hanna Seikkula: thanks for all the unforgettable moments in the laboratory and particularly outside the laboratory. Those moments have made this a pleasant journey. I also want to thank Miika Lehtinen, Juha Seikkula, Jori Jurttila, Pauliina Luoto, Henri Sipilä, Viki-Veikko Elomaa, and Cheng-Bin Yim.

Finally, I owe my deepest thanks to my family Sanne, Nia, and Ari-Pekka, to my mother Sirpa and to my brother Niko and his family. Without you, there is nothing.

This work was financially supported by the Turku University Foundation, the Academy of Finland, and the Finnish Society of Nuclear Medicine.

Turku, January, 2012

9. REFERENCES

Adam MJ, Grierson JR, Ruth TJ, Jivan S. Reaction of [^{18}F]acetyl hypofluorite with derivatives of dihydroxyphenylalanine: synthesis of L-[^{18}F]6-fluorodopa. Int J Radiat Appl Instrum Appl Radiat Isot 1986a; 37:877-82.

Adam MJ, Ruth TJ, Grierson JR, Abeysekera B, Pate BD. Routine synthesis of L-[^{18}F]6-fluorodopa with fluorine-18 acetyl hypofluorite. J Nucl Med 1986b; 27:1462-6.

Adam MJ, Jivan S. Synthesis and purification of L-6-[^{18}F]fluorodopa. Int J Radiat Appl Instrum Appl Radiat Isot 1988; 39:1203-6.

Akita K, Yoshida F. Bubble size, interfacial area, and liquid-phase mass transfer coefficient in bubble columns. Ind Eng Chem, Process Des Develop 1974; 13:84-91.

Andreasen NC. Brain Imaging: applications in psychiatry. Science 1988; 239:1381-1388.

Annesley TM. Ion suppression in mass spectrometry. Clin Chem 2003;49:1041-1044.

Aquilonius SM, Bergström K, Eckernäs SA, Hartvig P, Leenders KL, Lundquist H, Antoni G, Gee A, Rimland A, Uhlin J, et al. *In vivo* evaluation of striatal dopamine reuptake sites using ^{11}C-nomifensine and positron emission tomography. Acta Neurol Scand 1987; 76:283-7.

Barrio JR, Huang SC, Yu DC, Melega WP, Quintana J, Cherry SR, Jacobson A, Namavari M, Satyamurthy N, Phelps ME. Radiofluorinated L-m-tyrosines: new *in vivo* probes for central dopamine biochemistry. J Cereb Blood Flow Metab 1996; 16:667-78.

Becherer A, Szabo M, Karanikas G, Wunderbaldinger P, Angelberger P, Raderer M, Kurtaran A, Dudczak R, Kletter K. Imaging of advanced neuroendocrine tumors with ^{18}F-FDOPA PET. J Nucl Med 2004; 45:1161-7.

Bell C. Peripheral dopaminergic nerves. Pharmacol Ther 1989; 44:157-79.

Bergman J, Haaparanta M, Solin O. A novel radioisotope labelled compound, a mixture comprising said compound and a method for its preparation. Finnish Patent 96603, WO 96/20940.

Bergman J, Solin O. ^{18}Fluorine-labeled fluorine gas for synthesis of tracer molecules. Nucl Med Biol 1997; 24:677-83.

Bergström KA, Halldin C, Kuikka JT, Swahn C-G, Tiihonen J, Hiltunen J, Länsimies E, Farde L. Lipophilic metabolite of [^{123}I]β-CIT in human plasma may obstruct quantitation of the dopamine transporter. Synapse 1995; 19:297-300.

Berridge MS, Apana SM, Hersh JM. Teflon radiolysis as the major source of carrier in fluorine-18. J Label Compd Radiopharm 2009; 52:543-8.

Blessing G, Coenen HH, Franken K, Qaim SM. Production of [^{18}F]F_2, H^{18}F and $^{18}F_{aq}^-$ using the ^{20}Ne(d, α)^{18}F process. Appl Radiat Isot 1986; 37:1135-9.

von Bohlen und Halbach O. Dermietzel R. Neurotransmitters and neuromodulators, Handbook of receptors and biological effects. 2006 2nd edition, Wiley-VCH Verlag GmbH & Co. KGaA, Weinheim.

Cai L, Lu S, Pike VW. Chemistry with [^{18}F]fluoride ion. Eur J Org Chem 2008; 2853-73.

Canfield DR, Spelman RD, Kaufman MJ, Madras BK. Autoradiographic localization of cocaine binding sites by [^{3}H]CFT ([^{3}H]WIN 35,428) in the monkey brain. Synapse 1990; 6:189-95.

Carlsson A, Lindqvist M, Magnusson T, Waldeck B. On the presence of 3-hydroxytyramine in brain. Science 1958; 127:471.

Casella V, Ido T, Wolf AP, Fowler JS, MacGegor RR, Ruth TJ. Anhydrous ^{18}F labeled elemental fluorine for radiopharmaceutical preparation. J Nucl Med 1980; 21:750-757.

Chaly T, Diksic M. High Yield Synthesis of 6-[^{18}F]fluoro-L-dopa by regioselective fluorination of protected L-dopa with [^{18}F]acetylhypofluorite. J Nucl Med 1986; 27:1896-901.

Chirakal R, Firnau G, Schrobilgen GJ, McKay J, Garnett ES. The synthesis of [^{18}F]xenon difluoride from [^{18}F]fluorine gas. Int Appl Radiat Isot 1984a; 35:401-4.

Chirakal R, Firnau G, Cousea J, Garnetta E.S: Radiofluorination with ^{18}F-labelled acetyl hypofluorite: [^{18}F]-L-6-fluorodopa. Int J Appl Radiat. Isot 1984b; 35:651-3.

Chirakal R, Firnau G, Garnett E.S: High yield synthesis of 6-[^{18}F]fluoro-L-dopa. J Nucl Med 1986; 27:417-21.

Chirakal R, Adams R.M, Firnau G, Schrobilgen G.J., Coates G, Garnett E.S.: Electrophilic ^{18}F from a Siemens 11 MeV proton-only cyclotron. Nucl Med Biol 1995; 22:111-6.

Chitneni SK, Garreau L, Cleynhens B, Evens N, Bex M, Vermaelen P, Chalon S, Busson R, Guilloteau D, Van Laere K, Verbruggen A, Bormans G. Improved synthesis and metabolic stability analysis of the dopamine transporter ligand [^{18}F]FECT. Nucl Med Biol 2008; 35:75-82.

Clarke RL, Daum SJ, Gambino AJ, Aceto MD, Pearl J, Levitt M, Cumiskey WR, Bogado EF. Compounds affecting the central nervous system. 4.3β-Phenyltropane-2-carboxylic esters and analogs. J Med Chem 1973; 16:1260-7.

Coenen HH, Moerlein SM. Regiospecific aromatic fluorodemetallation of group IVb metalloarenes using elemental fluorine or acetyl hypofluorite. J Fluorine Chem 1987; 36:63-75.

Coenen HH, Franken K, Kling P, Stöcklin G. Direct electrophilic radiofluorination of phenylalanine, tyrosine and dopa. Appl Radiat Isot 1988; 39:1243-50.

Coenen HH. Fluorine-18 labeling methods: Features and possibilities of basic reactions, in Ernst Schering Research Foundation Workshop 62; PET Chemistry eds. Schubiger PA, Lehmann L, Friebe M. Springer-Verlag Berlin Heidelberg 2007; chapter 2:15-50.

Cooper JR, Bloom FE, Roth RH. Dopamine, in The biochemical basis of neuropharmacology. Oxford University Press New York 1996; 293-351.

Creveling CR. Kirk KL. (1985) The effect of ring-fluorination on the rate of O-methylation of dihydroxyphenylalanine (DOPA) by catechol-O-methyltransferase: significance in the development of ^{18}F-PETT scanning agents. Biochem Biophys Res Commun 1985; 130:1123-31.

Cropley VL, Fujita M, Innis RB, Nathan PJ. Molecular imaging of the dopaminergic system and its association with human cognitive function. Biol Psychiatry 2006; 59:898-907.

Dannals RF, Neumeyer JL, Milius RA, Ravert HT, Wilson AA, Wagner HN. Synthesis of a radiotracer for studying dopamine uptake sites *in vivo* using PET 2-β-carbomethoxy-3-β-(4-fluorophenyl)-[N-^{11}C-methyl]tropane ([^{11}C]CFT or [^{11}C]WIN-35,428). J Label Compd Radiopharm 1993; 33:147-52.

DeJesus OT. Positron-labeled DOPA analogs to image dopamine terminals. Drug Dev Research 2003; 59:249-60.

Diksic M, Farrokhzad S. New synthesis of ^{18}fluorine-labeled 6-fluoro-L-dopa by cleaving the carbon-silicon bond with fluorine. J Nucl Med 1985; 26:1314-18.

Dolbier Jr WR, Li A-R, Koch CJ, Shiue C-Y, Kachur AV. [^{18}F]EF5, a marker for PET detection of hypoxia: Synthesis of precursor and a new fluorination procedure. Appl Radiat Isot 2001; 54:73-80.

Dollé F, Demphel S, Hinnen F, Fournier D, Vaufrey F, Crouzel C. 6-[^{18}F]Fluoro-L-DOPA by radiofluorodestannylation: A Short and simple synthesis of a new labelling precursor. J. Labelled Comp Radiopharm 1998; 41:105-14.

Dollé F, Emond P, Mavel S, Demphel S, Hinnen F, Mincheva Z, Saba W, Valette H, Chalon S, Halldin C, Helfenbein J, Legaillard J, Madelmont JC, Deloye JB, Bottlaender M, Guilloteau D. Synthesis, radiosynthesis and *in vivo* preliminary evaluation of [^{11}C]LBT-999, a selective radioligand for the visualisation of the dopamine transporter with PET. Bioorg Med Chem 2006; 14:1115-25.

Doudet DJ, Chan GL, Jivan S, DeJesus OT, McGeer EG, English C, Ruth TJ, Holden JE. Evaluation of dopaminergic presynaptic integrity: 6-[^{18}F]fluoro-L-dopa versus 6-[^{18}F]fluoro-L-m-tyrosine. J Cereb Blood Flow Metab 1999; 19:278-87.

Eberling JL, Bankiewicz KS, O'Neil JP, Jagust WJ. PET 6-[^{18}F]fluoro-L-m-tyrosine studies of dopaminergic function in human and nonhuman primates. Front Hum Neurosci 2007;1:9.

Eisenhofer G. The role of neuronal and extraneuronal plasma membrane transporters in the inactivation of peripheral catecholamines. Pharmacol Ther 2001; 91:35-62.

Elsinga PH, Hatano K, Ishiwata K. PET tracers for imaging of the dopaminergic system. Curr Med Chem 2006; 13:2139-53.

Elsinga P, Todde S, Penuelas I, Meyer G, Farstad B, Faivre-Chauvet A, Mikolajczak R, Westera G, Gmeiner-Stopar T, Decristoforo C, The Radiopharmacy Committee of the EANM. Guidance on current good radiopharmacy practice (cGRPP) for the small-scale preparation of radiopharmaceuticals. Eur J Nucl Med Mol Imaging 2010; 37:1049–62.

Eskola O, Grönroos TJ, Forsback S, Tuomela J, Komar G, Bergman J, Härkönen P, Haaparanta M, Minn H, Solin O. Tracer level electrophilic synthesis and pharmacokinetics of the hypoxia tracer [^{18}F]EF5. MIB 2011; DOI: 10.1007/s11307-011-0484-4.

Farde L, Halldin C, Müller L, Suhara T, Karlsson P, Hall H. PET Study of [^{11}C]*β*-CIT binding to monoamine transporters in the monkey and human brain. Synapse 1994; 16:93-103.

Firnau G, Nahmias C, Garnett S. The preparation of [^{18}F]5-fluoro-DOPA with reactor-produced fluorine-18. Int J Appl Radiat Isot 1973; 24:182-4.

Firnau G, Chirakal R, Sood S, Garnett S. Aromatic fluorination with xenon difluoride: L-3,4-dihydroxy-6-fluoro-phenylalanine. Can J Chem 1980; 58:1449-50.

Firnau, G., Chirakal, R., Garnett, E.S.: Aromatic radiofluorination with [^{18}F]fluorine gas: 6-[^{18}F]fluoro-L-DOPA. J Nucl Med 1984; 25:1228-33.

Firnau G, Garnett ES, Chirakal R, Sood S, Nahmias C, Schrobilgen G. [^{18}F]Fluoro-L-dopa for the *in vivo* study of intracerebral dopamine. Int J Rad Appl Instrum A 1986; 37:669-75.

Firnau G, Sood S, Chirakal R, Nahmias C, Garnett ES. Cerebral metabolism of 6-[^{18}F]fluoro-L-3,4-dihydroxyphenylalanine in the primate. J Neurochem 1987; 48:1077-82.

Fowler JS, Shiue CY, Wolf AP, Salvador PA, MacGregor RR. Synthesis of ^{18}F-labeled acetylhypofluorite for radiotracer synthesis. J Label Compd Radiopharm 1982; 19:1634-6.

Freeby M, Goland R, Ichise M, Maffei A, Leibel R, Harris P. VMAT2 quantitation by PET as a biomarker for beta-cell mass in health and disease. Diabetes Obes Metab 2008; 10:98-108.

Frost JJ, Rosier AJ, Reich SG, Smith JS, Ehlers MD, Snyder SH, Ravert HT, Dannals RF. Positron emission tomographic imaging of the dopamine transporter with ^{11}C-WIN 35,428 reveals marked declines in mild Parkinson's disease. Ann Neurol 1993; 34:423–31.

Füchtner, F., Angelberger, P., Kvaternik, H., Hammerschmidt, F., Peric Simovc, B., Steinbach, J. Aspects of 6-[^{18}F]Fluoro-L-DOPA preparation: Precursor synthesis, preparative HPLC purification and determination of radiochemical purity. Nucl Med Biol 2002; 29:477-81.

Füchtner F, Zessin J, Mäding P, Wüst F. Aspects of 6-[^{18}F]fluoro-L-DOPA preparation - Deuterochloroform as a substitute solvent for Freon 11. Nuklearmedizin 2008; 47:62–4.

Füchtner F, Preusche P, Mäding P, Zessin J, Steinbach J. Factors affecting the specific activity of [^{18}F]fluoride from a [^{18}O]water target. Nuklearmedizin 2008; 47:116-9.

Garnett ES, Firnau G, Chan PKH, Sood S, Belbeck LW. [^{18}F]Fluoro-dopa, an analogue of dopa, and its use in direct external measurements of storage, degradation and turnover of intracerebral dopamine. Proc Natl Acad Sci USA 1978; 75:464-7.

Garnett, E.S., Firnau, G., Nahmias C.: Dopamine visualized in the basal ganglia of living man. Nature 1983; 305:137-8.

Goodman MM, Kilts CD, Keil R, Shi B, Martarello L, Xing D, Votaw J, Ely TD, Lambert P, Owens MJ, Camp VM, Malveaux E, Hoffman JM. ^{18}F-labeled FECNT: a selective radioligand for PET imaging of brain dopamine transporters. Nucl Med Biol 2000; 27:1-12.

Goswami R, Ponde DE, Kung MP, Hou C, Kilbourn MR, Kung HF. Fluoroalkyl derivatives of dihydrotetrabenazine as positron emission tomography imaging agents targeting vesicular monoamine transporters. Nucl Med Biol 2006; 33:685-94.

Guillaume M, Luxen A, Nebeling B, Argentini M, Clark JC, Pike VW. Recommendations for fluorine-18 production. Appl Radiat Isot 1991; 42:749-762.

Haaparanta M, Bergman J, Laakso A, Hietala J, Solin O. [^{18}F]CFT ([^{18}F]WIN 35,428), a radioligand to study the dopamine transporter with PET: biodistribution in rats. Synapse. 1996; 23:321-7.

Haaparanta M, Grönroos T, Marjamäki P, Eskola O, Bergman J, Paul R, Solin O. *In vivo* sampling for pharmacokinetic studies in small experimental animals: a combination of microdialysis, planar chromatography and digital autoradiography. Mol Imaging Biol 2004; 6:27-33.

Hantraye P, Brownell AL, Elmaleh D, Spealman RD, Wullner U, Brownell GL, Madras BK, Isacson O. Dopamine fiber detection by [^{11}C] CFT and PET in a primate model of Parkinsonism. Neuroreport 1992; 3:265-8.

Harada N, Nishiyama S, Satoh K, Fukumoto D, Kakiuchi T, Tsukada H. Age-related changes in the striatal dopaminergic system in the living brain: A Multiparametric PET study in conscious monkeys. Synapse 2002; 45:38-45.

Harada N, Ohba H, Fukumoto D, Kakiuchi T, Tsukada H. Potential of [^{18}F]beta-CFT-FE (2beta-carbomethoxy-3beta-(4-fluorophenyl)-8-(2-[^{18}F]fluoroethyl)nortropane) as a dopamine transporter ligand: A PET study in the conscious monkey brain. Synapse 2004; 54:37-45.

Hartvig P, Lindner KJ, Tedroff J, Andersson Y, Bjurling P, Långström B. Brain kinetics of ^{11}C-labelled L-tryptophan and 5-hydroxy-L-tryptophan in the rhesus monkey. A Study using positron emission tomography. J Neural Transm Gen Sect 1992; 88:1-10.

Hatano K, Ishiwata K, Yanagisawa T. Co production of 2,6-[^{18}F] difluoroDOPA during electrophilic synthesis of 6-[^{18}F]fluoro-L-DOPA. Nucl Med Biol 1996; 23:101-3.

Heikkila RE, Cabbat FS, Manzino L, Duvoisin RC. Rotational behavior induced by cocaine analogs in rats with unilateral 6-hydroxydopamine lesions of the substantia nigra: Dependence Upon Dopamine Uptake Inhibition. J Pharmacol Exp Ther 1979; 211:189-94.

Hiller A, Fischer C, Jordanova A, Patt JT, Steinbach J. Investigations to the synthesis of n.c.a. [^{18}F]$FClO_3$ as electrophilic fluorinating agent. Appl Radiat Isot 2008; 66:152-7.

Hoffman BJ, Hansson SR, Mezey É, Palkovits M. Localization and dynamic regulation of biogenic amine transporters in the mammalian central nervous system. Front Neuroendocrinol 1998; 19:187-231.

Hoffman JM, Melega WP, Hawk TC, Grafton TC, Luxen A, Mahoney DK, Barrio JR, Huang S-C, Maziotta JC, Phelps ME. The Effects of carbidopa administration on 6-[^{18}F]fluoro-L-DOPA kinetics in positron emission tomography. J Nucl Med 1992; 33:1472-7.

Hsu SM, Raine L. Protein A, avidin, and biotin in immunohistochemistry. J Histochem Cytochem 1981; 29:349-53.

Hsu SM, Raine L, Fanger H. The use of antiavidin antibody and avidin-biotin-peroxidase complex in immunoperoxidase technics. Am J Clin Pathol 1981; 75:816-21.

Hume SP, Myers R. Dedicated small animal scanners: a new tool for drug development? Curr Pharm Des 2002; 8:1497-511.

Ichise M, Harris PE. Imaging of beta-Cell Mass and Function. J Nucl Med 2010; 51:1001-4.

International Commission on Radiological Protection. The 2007 Recommendations. Ann ICRP 2007; 37:2-4.

Ishiwata K, Ishii S-I, Senda M, Tsuchiya Y, Tomimoto K. Electrophilic synthesis of 6-[^{18}F]fluoro-l-dopa: Use of 4-O-pivaloyl-l-dopa as a suitable precursor for routine production. Appl Radiat Isot 1993; 44:755-59.

Ishiwata K, Ogi N, Tanaka A, Senda M. Quantitative *ex vivo* and *in vitro* receptor autoradiography using ^{11}C-labeled ligands and an imaging plate: a study with a dopamine D2-like receptor ligand [^{11}C]nemonapride. Nucl Med Biol 1999; 26:291-6.

Iversen L. Neurotransmitter transporters: fruitful targets for CNS drug discovery. Mol Psychiatry 2000; 5:357-62.

Jacobs AH, Li H, Winkeler A, Hilker R, Knoess C, Rüger A, Galldiks N, Schaller B, Sobesky J, Kracht L, Monfared P, Klein M, Vollmar S, Bauer B, Wagner R, Graf R, Wienhard K, Herholz K, Heiss WD. PET-based molecular imaging in neuroscience. Eur J Nucl Med Mol Imaging 2003; 30:1051-65.

Johansson L, Mattsson S, Nosslin B, Leide-Svegborn S. Effective dose from radiopharmaceuticals. Eur J Nucl Med Mol Imag 1992; 19:933-8.

Johnston RF, Pickett SC, Barker DL. Autoradiography using storage phosphor technology. Electrophoresis 1990; 11:355-60.

Kaneko S, Ishiwata K, Hatano K, Omura H, Ito K, Senda M. Enzymatic synthesis of no-carrier-added 6-[^{18}F]fluoro-L-dopa with β-tyrosinase. Appl Radiat Isot 1999; 50:1025-32.

Kao C-HK, Hsu W-L, Xie H-L, Lin M-CL, Lan W-C, Chao H-Y. GMP production of [^{18}F]FDOPA and issues concerning its quality analyses as in USP "Fluorodopa F 18 Injection". Ann Nucl Med 2011; 25:309-16.

Kaufman MJ, Madras BK. Severe depletion of cocaine recognition sites associated with the dopamine transporter in parkinson's-diseased Striatum. Synapse 1991; 9:43-9.

Kaufman MJ, Spelman RD, Madras BK. Distribution of cocaine recognition sites in monkey brain: I. *In Vitro* Autoradiography with [^{3}H]CFT. Synapse 1991; 9:177-87.

Kaufman MJ, Madras BK. Distribution of cocaine recognition sites in monkey brain: II. *Ex vivo* Autoradiography with [^{3}H]CFT and [^{125}I]RTI-55. Synapse 1992; 12:99-111.

Kaufman MJ, Madras BK. [^{3}H]CFT ([^{3}H]WIN 35,428) accumulation in dopamine regions of monkey brain: comparison of a mature and an aged monkey. Brain Res 1993; 611:322-5.

Kilbourn MR, Sherman PS, Pisani T. Repeated reserpine administration reduces *in vivo* [^{18}F]GBR 13119 binding to the dopamine uptake site. Eur J Pharmacol 1992; 216:109-12.

Kilbourn MR, DaSilva JN, Frey KA, Koeppe RA, Kuhl DE. *In vivo* imaging of vesicular monoamine transporters in human brain using [^{11}C]tetrabenazine and positron emission tomography. J Neurochem 1993; 60:2315-8.

Kirschner A, Ice R, Beierwaltes W. Radiation dosimetry of ^{131}I-19-iodocholesterol: the pitfalls of using tissue concentration data [author reply]. J Nucl Med 1975; 16:248-9.

Koivula T, Marjamäki P, Haaparanta M, Fagerholm V, Grönroos T, Lipponen T, Perhola O, Vepsäläinen J, Solin O. *Ex vivo* evaluation of N-(3-[^{18}F]fluoropropyl)-2β-carbomethoxy-3β-(4-fluorophenyl)nortropane in rats. Nucl Med Biol 2008; 35:177-83.

Koopmans KP, Neels ON, Kema IP, Elsinga PH, Links TP, de Vries EG, Jager PL. Molecular imaging in neuroendocrine tumors: molecular uptake mechanisms and clinical results. Crit Rev Oncol Hematol 2009; 71:199-213.

Krasikova RN, Zaitsev VV, Ametamey SM, Kuznetsova OF, Fedorova OS, Mosevich IK, Belokon YN, Vyskočild Š, Shatik SV, Nader M, Schubiger PA. Catalytic enantioselective synthesis of ^{18}F-fluorinated α-amino acids under phase-transfer conditions using (*S*)-NOBIN. Nucl Med Biol 2004; 31:597-603.

Krasikova RN, Kuznetsova OF, Fedorova OS, Mosevich IK, Maleev VI, Belokon Yu N, Savel'eva TF, Sagiyan AS, Dadayan SA, Petrosyan AA. Asymmetric synthesis of 6-^{18}F-*L*-FDOPA using chiral Nickel(II) complexes. Radiochem 2007; 49:449-54.

Kuikka JT, Bergström KA, Vanninen E, Laulumaa V, Hartikainen P, Länsimies E. Initial experience with single-photon emission tomography using iodine-123-labelled 2-β-carbomethoxy-3-β-(4-iodophenyl)tropane in human brain. Eur J Nucl Med 1993; 20:783-6.

Kumakura Y, Cumming P. PET studies of cerebral levodopa metabolism: a review of clinical findings and modeling approaches. Neuroscientist 2009; 15:635-50.

Kung HF, Lieberman BP, Zhuang ZP, Oya S, Kung MP, Choi SR, Poessl K, Blankemeyer E, Hou C, Skovronsky D, Kilbourn M. *In vivo* imaging of vesicular monoamine transporter 2 in pancreas using an ^{18}F epoxide derivative of tetrabenazine. Nucl Med Biol 2008; 35:825-37.

Kämäräinen E, Kyllönen T, Airaksinen A, Lundkvist C, Yu M, Någren K, Sandell J, Langer O, Vepsäläinen J, Hiltunen J, Bergström K, Lötjönen S, Jaakkola T, Halldin C. Preparation of [^{18}F]beta-CFT-FP and [^{11}C]beta-CFT-FP, selective radioligands for visualisation of the dopamine transporter using positron emission tomography (PET) J Label Compd Radiopharm 2000; 43:1235-44.

Laakso A, Bergman J, Haaparanta M, Vilkman H, Solin O, Hietala J. [^{18}F]CFT [(^{18}F)WIN 35,428], a radioligand to study the dopamine transporter with PET: characterization in human subjects. Synapse 1998; 28:244-50.

Laakso A, Hietala J. PET studies of brain monoamine transporters. Curr Pharm Des 2000; 6:1611-23.

Laakso A, Vilkman H, Alakare B, Haaparanta M, Bergman J, Solin O, Peurasaari J, Räkköläinen V, Syvälahti E, Hietala J. Striatal dopamine transporter binding in neuroleptic-naive patients with schizophrenia studied with positron emission tomography. Am J Psychiatry 2000a; 157:269-71.

Laakso A, Vilkman H, Kajander J, Bergman J, Haaparanta M, Solin O, Hietala J. Prediction of detached personality in healthy subjects by low dopamine transporter binding. Am J Psychiatry 2000b; 157:290-2.

Laakso A, Bergman J, Haaparanta M, Vilkman H, Solin O, Syvälahti E, Hietala J. Decreased striatal dopamine transporter binding *in vivo* in chronic schizophrenia. Schizophr Res 2001; 52:115-20.

Lambrecht RM, Neirinckx R, Wolf AP. Cyclotron isotopes and radiopharmaceuticals-XXIII. Novel anhydrous ^{18}F-fluorinating intermediates. Int J Radiat Appl Instrum Appl Radiat Isot 1978; 29:175-183.

Lasne M-C, Perrio C, Rouden J, Barré L, Roeda D, Dollé F, Crouzel C. Chemistry of β^+-emitting compounds based on fluorine-18. Top Curr Chem 2002; 222:201-58.

Lee CM, Farde L. Using positron emission tomography to facilitate CNS drug development. Trends Pharmacol Sci 2006; 27:310-6.

Lee CS, Samii A, Sossi V, Ruth TJ, Schulzer M, Holden JE, Wudel J, Pal PK, De La Fuente-Fernandez R, Calne DB, Stoess AJ. *In vivo* positron emission tomographic evidence for compensatory changes in presynaptic dopaminergic nerve terminals in Parkinson's disease. Ann Neurol 2000; 47:493–503.

Lemaire C, Guillaume M, Cantineau R, Christiaens L. No-carrier-added regioselective preparation of 6-[^{18}F]fluoro-L-dopa. J Nucl Med 1990; 31:1247-51.

Lemaire C, Guillaume M, Cantineau R, Plenevaux A, Christiaens L. An approach to the asymmetric synthesis of L-6-[^{18}F]fluorodopa via NCA nucleophilic fluorination. Appl Radiat Isot 1991; 42:629-35.

Lemaire C, Plenevaux A, Cantineau R, Christiaens L, Guillaume M, Comar D. Nucleophilic

enantioselective synthesis of 6-[^{18}F]fluoro-L-dopa via two chiral auxiliaries. Appl Radiat Isot 1993; 44:737-44.

Lemaire, C., Damhaut, P., Plenevaux, A., Comar, D. Enantioselective synthesis of 6-[^{18}F]-fluoro-L-dopa from no-carrier-added Fluorine-18-Fluoride. J Nucl Med 1994; 35:1996-2002.

Lemaire C, Gillet S, Guillouet S, Plenevaux A, Aerts J, Luxen A. Highly enantioselective synthesis of no-carrier-added 6-[^{18}F]fluoro-L-dopa by chiral phase-transfer alkylation. Eur J Org Chem 2004:2899-904.

Loc'h C, Müller L, Ottaviani M, Halldin C, Farde L, Maziere M. Synthesis of 2β-carbomethoxy-3β-(4-[^{76}Br]bromophenyl)tropane ([^{76}Br]β-CBT), a pet tracer for *in vivo* imaging of the dopamine uptake sites. J Lab Comp Radiopharm 1995; 36:385-92.

Luxen, A., Perlmutter, M., Bida, G.T., Van Moffaert, G., Cook J.S., Satyamurthy, N., Phelps, M.E., Barrio, J.R.: Remote, semiautomated production of 6-[^{18}F]fluoro-L-DOPA for human studies with PET. Appl Radiat Isot 1990; 41:275-81.

Luxen A, Guillaume M, Melega W P, Pike V W, Solin O, Wagner R. Production of 6-[^{18}F]fluoro-L-DOPA and its metabolism *In Vivo* - a Critical Review. Nucl Med Biol 1992; 2:149-58.

Ma Y, Dhawan V, Mentis M, Chaly T, Spetsieris PG, Eidelberg D. Parametric mapping of [^{18}F]FPCIT binding in early stage Parkinson's disease: a PET study. Synapse. 2002; 45:125-33.

Marjamaki P, Haaparanta M, Forsback S, Fagerholm V, Eskola O, Gronroos T, Koivula T, Solin O. Comparison of 2β-carbomethoxy-3β-(4-[^{18}F]fluorophenyl)tropane and N-(3-[^{18}F]fluoropropyl)-2β-carbomethoxy-3β-(4-fluorophenyl)nortropane, Tracers for imaging dopamine transporter in rat. Mol Imag Biol 2009; 12:269-77.

Mason NS, Mathis CA. Radiohalogens for PET Imaging, in positron emission tomography – Basic science and clinical practice. Eds. Valk PE, Bailey DL, Townsend DW, Maisey MN. Springer-Verlag, London 2003;chapter 9:217-36.

Maziere B, Loc'h C, Müller L, Halldin CH. ^{76}Br-*β*-CBT, a PET tracer for investigating dopamine neuronal uptake. Nucl Med Biol 1995; 22:993-7.

Melega WP, Luxen A, Perlmutter MM, Nissenson CHK, Phelps ME, Barrio JR. Comparative *in vivo* metabolism of 6-[^{18}F]fluoro-L-dopa and [^{3}H]L-dopa in rats. Biochem Pharmacol 1990; 39:1853-60.

Meltzer PC, Liang AY, Brownell A-L, Elmaleh DR, Mardas BK. Substituted 3-phenyltropane analogs of cocaine: synthesis, inhibition of binding at cocaine recognition sites, and positron emission tomography imaging. J Med Chem 1993; 36:855-62.

Minn H, Kauhanen S, Seppänen M, Nuutila P. ^{18}F-FDOPA: a multiple-target molecule. J Nucl Med 2009; 50:1915-8.

Morón JA, Brockington A, Wise RA, Rocha BA, Hope BT. Dopamine uptake through the norepinephrine transporter in brain regions with low levels of the dopamine transporter: evidence from knock-out mouse lines. J Neurosci 2002; 22:389-95.

Müller L, Halldin C, Farde L, Karlsson P, Hall H, Swahn C-G, Neumeyer J, Gao Y, Milius R. [^{11}C]*β*-CIT, a cocaine analogue. Preparation, autoradiography and preliminary PET investigation. Nucl Med Biol 1993; 20:249-55.

Najafi A. Measures and pitfalls for successful preparation of "no carrier added" asymmetric 6-[^{18}F]fluor-l-dopa from ^{18}F-fluoride ion. Nucl Med Biol 1995; 22:395-7.

Nakao R, Furutsuka K, Yamaguchi M, Suzuki K. Sensitive determination of specific radioactivity of positron emission tomography radiopharmaceuticals by radio high-performance liquid chromatography with fluorescence detection. Nucl Med Biol 2008; 35:733-40.

Namavari M, Bishop A, Satymurthy N, Bida G, Barrio J.R. Regioselective radiofluoro-destannylation with [^{18}F]F_2 and [^{18}F]CH_3COOF: a high yield synthesis of 6-[^{18}F]fluoro-L-dopa. Appl Radiat Isot 1992; 43:989-96.

Neumeyer JL, Wang S, Milius RA, Baldwin RM, Zea-Ponce Y, Hoffer PB, Sybirska E, Al-Tikriti M, Charney DS. [^{123}I]-2β-carbomethoxy-3β-(4-iodophenyl)tropane: high-affinity SPECT (single photon emission computed tomography) radiotracer of monoamine reuptake sites in brain. J Med Chem 1991; 34:3144-6.

Nickles RJ, Hichwa RD, Daube ME, Hutchins GD, Congdon DD. An $^{18}O_2$-target for the high yield production of [^{18}F]fluoride. Int J Appl Radiat Isot 1983; 34:625-29.

Nickles RJ, Daube ME, Ruth TJ. An $^{18}O_2$ target for the production of [^{18}F]F_2. Int J Appl Radiat Isot 1984; 35:117-22.

Nozaki S, Kato M, Takano H, Ito H, Takahashi H, Arakawa R, Okumura M, Fujimura Y, Matsumoto R, Ota M, Takano A, Otsuka A, Yasuno F, Okubo Y, Kashima H, Suhara T. Regional dopamine

synthesis in patients with schizophrenia using L-[β-^{11}C]DOPA PET. Schizophr Res 2009; 108:78-84.

Nurmi E, Ruottinen HM, Kaasinen V, Bergman J, Haaparanta M, Solin O, Rinne JO. Progression in Parkinson's disease: a positron emission tomography study with a dopamine transporter ligand [^{18}F]CFT. Ann Neurol 2000a; 47:804-8.

Nurmi E, Bergman J, Eskola O, Solin O, Hinkka SM, Sonninen P, Rinne JO. Reproducibility and effect of levodopa on dopamine transporter function measurements: a [^{18}F]CFT PET study. J Cereb Blood Flow Metab 2000b; 20:1604-9.

Nurmi E, Bergman J, Eskola O, Solin O, Vahlberg T, Sonninen P, Rinne JO. Progression of dopaminergic hypofunction in striatal subregions in Parkinson's disease using [^{18}F]CFT PET. Synapse 2003; 48:109-15.

Någren K, Halldin C, Müller L, Swahn C-G, Lehikoinen P. Comparison of [^{11}C]methyl triflate and [^{11}C]methyl iodide in the synthesis of PET radioligands such as [^{11}C]β-CIT and [^{11}C]β-CFT. Nucl Med Biol 1995; 22:965-70.

Oberdorfer F, Hofmann E, Maier-Borst W. Preparation of a new ^{18}F-labelled precursor: 1-[^{18}F]fluoro-2-pyridone. Appl Radiat Isot 1988; 39:685-8.

Okamura N, Villemagne VL, Drago J, Pejoska S, Dhamija RK, Mulligan RS, Ellis JR, Ackermann U, O'Keefe G, Jones G, Kung HF, Pontecorvo MJ, Skovronsky D, Rowe CC. *In vivo* measurement of vesicular monoamine transporter type 2 density in Parkinson disease with ^{18}F-AV-133. J Nucl Med 2010; 51:223-8.

Paans AMJ, van Waarde A, Elsinga PH, Willemsen ATM, Vaalburg W. Positron emission tomography: the conceptual idea using a multidisciplinary approach. Methods 2002; 27:195-207.

Park BK, Kitteringham NR. Effects of fluorine substitution on drug metabolism: pharmacological and toxicological implications. Drug Metab Rev 1994; 26:605-43.

Paxinos G, Watson C. The rat brain in stereotaxic coordinates. San Diego: Academic Press, 1986.

Piccini PP. Dopamine Transporter: Basic aspects and neuroimaging. Mov Disord 2003; 18:S3-8.

Poyot T, Conde F, Gregoire MC, Frouin V, Coulon C, Fuseau C, Hinnen F, Dollé F, Hantraye P, Bottlaender M. Anatomic and biochemical correlates of the dopamine transporter ligand ^{11}C-PE2I in normal and parkinsonian primates: Comparison with 6-[^{18}F]fluoro-L-dopa. J Cereb Blood Flow Metab 2001; 21:782-92.

Reddy GN, Haeberli M, Beer H-F, Schubiger AP. An improved synthesis of no-carrier-added (NCA) 6-[^{18}F]fluoro-L-DOPA and its remote routine production for PET investigations of dopaminergic systems. Appl. Radiat. Isot. 1993;44:645-9.

Ribeiro MJ, De Lonlay P, Delzescaux T, Boddaert N, Jaubert F, Bourgeois S, Dollé F, Nihoul-Fékété C, Syrota A, Brunelle F. Characterization of hyperinsulinism in infancy assessed with PET and ^{18}F-fluoro-L-DOPA. J Nucl Med 2005; 46:560-6.

Rinne JO, Bergman J, Ruottinen H, Haaparanta M, Eronen E, Oikonen V, Sonninen P, Solin O. Striatal uptake of a novel PET ligand, [^{18}F]β-CFT, is reduced in early Parkinson's disease. Synapse 1999a; 31:119-24.

Rinne JO, Ruottinen H, Bergman J, Haaparanta M, Sonninen P, Solin O. Usefulness of a dopamine transporter PET ligand [^{18}F]β-CFT in assessing disability in Parkinson's disease. J Neurol Neurosurg Psychiatry 1999b; 67:737-41.

Rinne JO, Nurmi E, Ruottinen HM, Bergman J, Eskola O, Solin O. [^{18}F]FDOPA and [^{18}F]CFT are both sensitive PET markers to detect presynaptic dopaminergic hypofunction in early Parkinson's disease. Synapse 2001; 40:193-200.

Robeson W, Dhawan V, Belakhlef A, Ma YL, Pillai V, Chaly T, Margouleff C, Bjelke D, Eidelberg D. Dosimetry of the dopamine transporter radioligand ^{18}F-FPCIT in human subjects. J Nucl Med 2003; 44:961-6.

Ruottinen HM, Rinne JO, Ruotsalainen UH, Bergman JR, Oikonen VJ, Haaparanta MT, Solin OH, Laihinen AO, Rinne UK. Striatal [^{18}F]fluorodopa utilization after COMT inhibition with entacapone studied with PET in advanced Parkinson's disease. J. Neural Transm Park Dis Dement Sect 1995; 10:91-106.

Ruth TJ, Wolf AP. Absolute cross sections for the production of ^{18}F via the ^{18}O(p,n)^{18}F reaction. Radiochim Acta 1979; 26:21-4.

Sarre S, Herregodts P, Deleu D, Devrieze A, Deklippel N, Ebinger G, Michotte Y. Biotransformation of L-DOPA in striatum and substantia nigra of rats with unilateral, nigrostriatal lesion: a microdialysis study. Naunyn Schmied Arch Pharmacol 1992; 346:277-85.

Satyamurthu N, Bida GT, Phelps ME, Barrio JR. *N*-[^{18}F]Fluoro-*N*-alkylsulfonamides: Novel reagents for mild and regioselective radiofluorination. Appl Radiat Isot 1990; 41:733-8.

Scheffel U, Pöğün S, Stathis M, Boja JW, Kuhar MJ. *In Vivo* Labeling of cocaine binding sites on

dopamine transporters with [^{3}H]WIN 35,428. J Pharmacol Exp Ther 1991; 257:954-8.

Schirrmacher R, Wängler C, Schirrmacher E. Recent Developments and trends in ^{18}F-radiochemistry: Syntheses and applications. Mini-Rev Org Chem 2007; 4:317-29.

Schirrmacher R, Wängler C, Schirrmacher E. Fluorine-18 radiochemistry: Theory and practice in Munich Molecular Imaging Handbook Series Volume 1 Scintomics, 2010:5-73.

Schlyer DJ. PET tracers and radiochemistry. Ann Acad Med Singapore 2004; 33:146-54.

Schnöckel U, Hermann S, Stegger L, Law M, Kuhlmann M, Schober O, Schäfers K, Schäfers M. Small-animal PET: A promising, non-invasive tool in pre-clinical research. Eur J Pharm Biopharm 2010; 74:50-4.

Schou M, Steiger C, Varrone A, Guilloteau D, Halldin C. Synthesis, radiolabeling and preliminary *in vivo* evaluation of [^{18}F]FE-PE2I, a new probe for the dopamine transporter. Bioorg Med Chem Lett 2009; 19:4843-5.

Schroeder J, Troe J. Elementary reactions in the gas-liquid transition range. Ann Rev Phys Chem 1987; 38:163-90.

Shen B, Ehrlichmann W, Uebele M, Machulla H-J, Reischl G. Automated synthesis of n.c.a. [^{18}F]FDOPA via nucleophilic aromatic substitution with [^{18}F]fluoride. App Radiat Isot 2009; 67:1650-3.

Sioka C, Fotopoulos A, Kyritsis AP. Recent advances in PET imaging for evaluation of Parkinson's disease. Eur J Nucl Med Mol Imaging 2010; 37:1594-603.

Solin O, Bergman J, Haaparanta M, Reissel A. Production of ^{18}F from water targets. Specific radioactivity and anionic contaminants. Appl Radiat Isot 1988; 39:1065-71.

Solin O, Eskola O, Hamill TG, Bergman J, Lehikoinen P, Grönroos T, Forsback S, Haaparanta M, Viljanen T, Ryan C, Gibson R, Kieczykowski G, Hietala J, Hargreaves R, Burns HD. Synthesis and characterization of a potent, selective, radiolabeled substance-P antagonist for NK1 receptor quantitation: ([^{18}F]SPA-RQ). Mol Imaging Biol 2004; 6:373-84.

Stabin MG, Sparks RB, Crowe E. OLINDA/EXM: the second-generation personal computer software for internal dose assessment in nuclear medicine. J Nucl Med 2005; 46:1023-27.

Stehouwer JS, Goodman MM. Fluorine-18 radiolabeled PET tracers for imaging monoamine transporters: Dopamine, serotonin, and norepinephrine. PET Clin. 2009; 4:101-28.

Strunecká A, Patočka J, Connett P. Fluorine in medicine. J Appl Biomed 2004; 2:141-50.

Szajek, L.P., Channing, M.A., Eckelman W.C. Automated Synthesis of 6-[^{18}F]fluoro-L- DOPA using modified polystyrene supports with bound 6-mercuric DOPA precursors. Appl. Radiat. Isot 1998; 49:795-804.

Teare H, Robins EG, Årstad E, Luthra SK, Gouverneur V. Synthesis and reactivity of [^{18}F]-*N*-fluorobenzenesulfonimide. Chem Commun 2007:2330-2.

Teare H, Robins EG, Kirjavainen A, Forsback S, Sandford G, Solin O, Luthra SK, Gouverneur V. Radiosynthesis and Evaluation of [^{18}F]Selectfluor bis(triflate). Angew Chem Int ed 2010; 49:6821-4.

Torres GE, Gainetdinov RR, Caron MG. Plasma membrane monoamine transporters: structure, regulation and function. Nat Rev Neurosci 2003; 4:13-25.

Tsao HH, Lin KJ, Juang JH, Skovronsky DM, Yen TC, Wey SP, Kung MP. Binding characteristics of 9-fluoropropyl-(+)-dihydrotetrabenzazine (AV-133) to the vesicular monoamine transporter type 2 in rats. Nucl Med Biol. 2010; 37:413-9.

Vallabhajosula S. Quality Control of PET Radiopharmaceuticals. Molecular imaging: radiopharmaceuticals for PET and SPECT. Springer-Verlag Berlin Heidelberg 2009;chapter 13:197-204.

Varrone A, Steiger C, Schou M, Takano A, Finnema SJ, Guilloteau D, Gulyás B, Halldin C. *In vitro* autoradiography and *in vivo* evaluation in cynomolgus monkey of [^{18}F]FE-PE2I, a new dopamine transporter PET radioligand. Synapse 2009; 10:871-80.

Verhoeff NP. Radiotracer imaging of dopaminergic transmission in neuropsychiatric disorders. Psychopharmacology (Berl) 1999; 147:217-49.

Volkow ND, Fowler JS, Gatley SJ, Logan J, Wang G-J, Ding Y-S, Dewey S. PET evaluation of the dopamine system of the human brain. J Nucl Med 1996; 37:1242-1256.

de Vries, E.F.J., Luurtsema, G., Brüssermann, M., Elsinga, P.H., Vaalburg, W.: Fully automated synthesis module for high yield one-pot preparation of 6-[^{18}F]Fluoro-L-DOPA. Appl Radiat Isot 1999; 51:389-94.

Wagner FM, Ermert J, Coenen HH. Three-step, "one-pot" radiosynthesis of 6-fluoro-3,4-dihydroxy-L-phenylalanine by isotopic exchange. J Nucl Med 2009; 50:1724-9.

Wilson A A, DaSilva J N, Houle S. *In vivo* evaluation of [^{11}C]- and [^{18}F]-labelled cocaine analogues as potential dopamine transporter ligands for positron emission tomography. Nucl Med Biol 1996; 23:141-6.

Wimalasena K. Vesicular monoamine transporters: Structure-function, pharmacology, and medicinal chemistry. Med Res Rev 2011; 31:483-519.

Wong DF, Yung B, Dannals RF, Shaya EK, Ravert HT, Chen CA, Chan B, Folio T, Scheffel U, Ricaurte GA, Neumeyer JL, Wagner HN jr, Kuhar MJ. *In vivo* imaging of baboon and human dopamine transporters by positron emission tomography using [^{11}C]WIN 35,428. Synapse 1993; 15:130-42.

Yin D, Zhang L, Tang G, Tang X, Wang Y. Enantioselective synthesis of no-carrier added (NCA) 6-[^{18}F]fluoro-L-dopa. J Radioanal Nucl Chem 2003; 257:179-85.

Yoder KK, Hutchins GD, Mock BH, Fei X, Winkle WL, Gitter BD, Territo PR, Zheng Q-H. Dopamine transporter binding in rat striatum: a comparison of [*O*-methyl-^{11}C]β-CFT and [*N*-methyl-^{11}C]β-CFT. Nucl Med Biol 2009; 36:11-6.

Zheng G, Dwoskin LP, Crooks PA. Vesicular monoamine transporter 2: role as a novel target for drug development. AAPS J 2006; 8:E682-92.

Zoghbi SS, Shetty HU, Ichise M, Fujita M, Imaizumi M, Liow JS, Shah J, Musachio JL, Pike VW, Innis RB. PET imaging of the dopamine transporter with ^{18}F-FECNT: a polar radiometabolite confounds brain radioligand measurements. J Nucl Med 2006; 47:520-7.